RSC Advances

This article can be cited before page numbers have been issued, to do this please use: K. L. Woon, Z. A. Hasan, B. K. Ong, A. Ariffin, R. Griniene, S. Grigalevicius and S. Chen, *RSC Adv.*, 2015, DOI: 10.1039/C5RA09340F.

ROYAL SOCIETY OF CHEMISTRY

www.rsc.org/advances

View Article Online
DOI: 10.1039/C5RA09340F

Table of contents entry

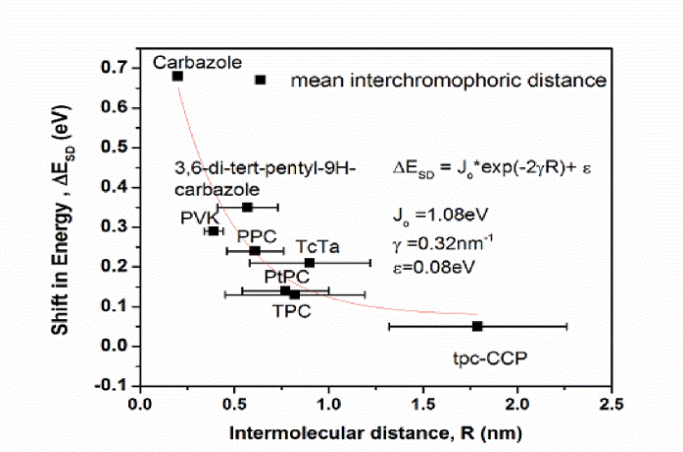

The red-shift of triplet energies between the dilute phase and solid states is a function of intermolecular distance.

View Article Online
DOI: 10.1039/C5RA09340F

Triplet states and Energy Back Transfer of Carbazole Derivatives

Kai Lin Woon[1,3*], Zainal A. Hasan[2,5] , Bee Kian Ong[2,5], Azhar Ariffin[2**], Raimonda Griniene[4] , Saulius Grigalevicius[4] , Show-An Chen[3]

[1]Low Dimensional Material Research Centre (LDMRC), Department of Physics, Faculty of Science, University of Malaya, 50603 Kuala Lumpur, Malaysia

[2]Department of Chemistry, Faculty of Science, University of Malaya, 50603 Kuala Lumpur, Malaysia

[3] Department of Chemical Engineering and Frontier Research Center on Fundamental and Applied Sciences of Matters, National Tsing-Hua University, 101, Section 2, Kuang-Fu Road, Hsinchu 30041, Taiwan, ROC

[4] Department of Polymer Chemistry and Technology, Kaunas University of Technology, Radvilenu Plentas 19, LT-50254 Kaunas, Lithuania

[5] ItraMAS Corporation. Sdn. Bhd., 542A-B Mukim 1, Lorong Perusahaan Baru 2, Kawasan Perindustrian Perai 13600, Penang, Malaysia

Correponding Authors *ph7klw76@um.edu.my , ** azhar70@um.edu.my

Abstract:

Intermolecular interactions among π conjugated semiconducting molecules often give rise to totally different optical behaviours between the solid states and dilute phases. Phosphorescence spectra observed in solid states are often lowered compared with dilute forms resulting in the red-shift of phosphorescence spectra. Here, we demonstrate that this red-shift can be reduced by introducing side groups. We also show that such a shift is a function of interchromophoric distance with fast exponential decay. Furthermore, we show conclusively that triplet exciton transfer between the hosts and the bis[2-(4F,6-difluorophenyl)pyridinato-C2,N](picolinato)iridium(III) can be described in terms of the Boltzmann factor using triplet energies obtained from the solid states. These results will have implications in molecular design that utilizes triplet excitons such as organic light emitting diodes and singlet fission solar cells.

View Article Online
DOI: 10.1039/C5RA09340F

Introduction

Triplet excitons are tightly bounded electron-hole pairs of total spin S = 1. These excitons have been used to provide efficient light emission in organic light emitting diodes (LEDs) [1-5] or to give free carriers in solar cells by dissociation of triplet excitons formed from singlet fission [6-8]. Triplet exciton confinement is a prerequisite for efficient phosphorescent organic LEDs[9-10]. In contrast with phosphorescent organic LEDs, singlet fission solar cells require a rapid triplet exciton transfer between two nearest neighbours but have a detrimental effect for the efficiency of organic phosphorescent LEDs[11]. In order to obtain highly efficient blue phosphorescent organic LEDs, hosts having high triplet energies are required. This is usually achieved by incorporating meso, insulating or twisted configurations into the molecular design[12]. However, interactions with other chromophores cannot be discounted in solid state devices and photosynthetic reaction centres[13-16]. The molecular interactions can include resonance, polarization, Van-der-Waals and exchange interactions for example[17]. When the strength of the interaction is particularly strong, a stable dimer may form. For a dimer, the mutual distance and orientation in the ground state and in the excited state is very similar. While for the excimer, the mutual distance and orientation between the excited and ground state equilibriums is significantly different. The strength of such interactions always depends on the intermolecular distance. Triplet energies of organic molecules are often determined in dilute forms in cryogenic temperatures[18-20]. Much consideration has been given to reducing the effective conjugations but little effort is given to understanding how intermolecular interactions can alter the energy levels. However, molecular interactions can red-shift and even completely change the spectra observed in solid states. These can give rise to triplet excimers such as in naphthalene[21,22] and carbazole systems[23,24]. Since most phosphorescent hosts are used in solid states, it is important to examine the phosphorescence spectra of such hosts in solid and dilute forms.

Depending on the strength of the interactions, the phosphorescence spectra of chromophores in a solid state is often red-shifted compared with the dilute forms. Despite the importance of molecular interactions, there has been little work done to study how short range interactions influence the observed phosphorescent spectra and how it differs from the dilute forms and the monomers. This maybe the result of vanishing small phosphorescent quantum yields from spin-forbidden transitions and increased non-radiative loss pathways in the solid state even at low temperatures[25]. Nevertheless, a greater understanding is required on how the intermolecular interactions can alter the observed phosphorescent spectra and their triplet energies. This is particularly relevant, for example, in determining the threshold

View Article Online
DOI: 10.1039/C5RA09340F

of triplet ionization in singlet fission solar cells[26], suppression of triplet excimers and effectiveness of triplet exciton confinement in phosphorescent LEDs. This study is carried out using a number of carefully selected organic semiconducting materials and their components, mainly carbazole based derivatives. The phosphorescent spectra obtained in solid states can be considered as a combination of interchromophore interaction and its contribution to the perturbation of the zero-order ("dilute") spectra. We report the difference between the spectra obtained in dilute forms and solid states. We show that such a red shift follows a fast exponential decay with distance. We go further to show how triplet energy transfer between bis[2-(4,6-difluorophenyl)pyridinato-C2,N](picolinato)iridium(III) (Firpic) and the host is affected.

Experimental Methods

Materials Synthesis

The synthesis of compounds **1 – 11** is shown in Scheme 1. The structures of intermediates and final products were confirmed by proton (^{1}H) and carbon (^{13}C) nuclear magnetic resonance (NMR) spectroscopy, infrared (IR) spectroscopy and mass spectrometry (MS). All commercially available starting materials, reagents and solvents were used as supplied, unless otherwise stated. All these materials were obtained from Aldrich or Merck. All reactions were carried out without exclusion of air unless otherwise stated and the temperatures were measured externally. Microwave irradiated reactions were performed in a CEM Microwave MARS 6, Xpress Plus vessel. For compounds with RMM < 800 g/mol mass spectra were recorded using a Schimadzu QP5050A gas chromatography/mass spectrometer with electron impact (EI) at a source temperature of 200 °C. For compounds with RMM > 800 g mol, mass spectra were analyzed using a Bruker reflex IV matrix-assisted laser desorption/ionization (MALDI) time-of-flight (TOF) MS. A 384-well microliter plate format was used with a scout target. Samples were dissolved in DCM with HABA (2-(4hydroxyphenylazo)benzoic acid) matrix (1:10 DCM:HABA). IR spectra were recorded using a Perkin-Elmer Spectrum 400 Fourier transform-infrared (FT-IR) Spectrometer, ^{1}H NMR and ^{13}C spectra were recorded using either a JEOL Lambda FT-400 spectrometer, Bruker Avance III FT-400 spectrometer or Bruker Avance III FT-600 MHz and an internal standard of tetramethylsilane (TMS). Aluminum-backed TLC plates coated with silica gel (60 F, Merck) were used to monitor the progress of reactions. Purification of intermediates and final products were performed by flash column chromatography, using silica gel 60 (0.063-0.200 mm) obtained from Merck. The experimental details are found in the Supporting Information. Poly{3,6-di(t-butyl)-9-[4-(3-methyloxetan-3-ylmethoxy)phenyl]carbazole} (**PtPC**) and poly{9-[4-(3-methyloxetan-3-

View Article Online
DOI: 10.1039/C5RA09340F

ylmethoxy)phenyl]carbazole} (**PPC**) are newly synthesized polymers. The chemical structures of the materials are given in Figure 1. The experimental details of the synthesis are provided in the Supporting Information. Poly(9-vinylcarbazole (**PVK**), 2,7-Bis(diphenylphosphoryl)-9,9'-spirobifluorene (**SPPO13**), 3,5-di(9H-carbazol-9-yl) tetraphenylsilane (**SIMCP2**) and 4,4′,4″-tris-(N-carbazolyl)-triphenlyamine (**TcTa**) are purchased from Lumtec.

Low Temperature Phosphorescent Spectra Measurement

Thin film samples were drop-casted onto a glass substrate heated at 60^{o}C from chloroform solution containing hosts at a concentration of 40 mg/mL. For a dilute system, the hosts are prepared at 0.1mg/ml dissolved in dichlorobenzene. The samples were attached to the sample holder in a nitrogen cryostat (Janis). The samples were excited at 350 nm by a 150 fs pulsed Ti:sapphire laser (Spectra-Physics Hurricane) at 1kHz repetition rate in conjunction with an ultrafast optical parametric amplifier (Quantronix TOPAS). The luminescence from the film was allowed to pass through a long pass filter (395nm) and a monochromator (Princeton Instruments Acton SP 2150) and then to a gated intensified CCD camera (Andor ICCD 334T). The intensified CCD was operated synchronously with gate delay of 100 μs for all samples with a detection window width of 850μs. To increase the signal to noise ratio, each final spectrum was obtained by averaging the accumulated spectra for at least 600,000 laser pulses with a gain of at least 100. The laser intensity was about 7 μJ/pulse. Measurements were carried out in a cryostat under vacuum of 10^{-7} Torr at 77 K for all samples. Origin 8.5 is used for the fitting. The spectra were fitted to Gaussian functions using least square regression. Good fitting is obtained when $R^2 > 0.99$ with the least number of Gaussian peaks. The locations of the first peaks were then extracted from the least square fitting.

Time Resolved Lifetime Measurement

Thin film samples (~200nm) were spin-coated from the chlorobenzene solutions containing the hosts and Firpic at a concentration of 1% by weight. The samples were excited at 400nm by a Ti:Sapphire laser using a similar set-up used for the determination of triplet energies. A synchronous delay of 20ns is used with a detection window of 20ns. Measurements were carried out in a cryostat (Janis) under vacuum of 10^{-7} Torr at 77 K for all samples. The time-resolved phosphorescence is measured up to 7μs.

Molecular Modelling and Molecular Dynamic Simulation

Gaussian 09 is used to model the torsional angle and potential barrier using the PM6 method at the ground state. For molecular dynamic simulations, the ground state molecular

View Article Online
DOI: 10.1039/C5RA09340F

configurations are optimized using the PM6 method to obtain the lowest energy conformer. For polymers, we duplicated the monomer and connected it back onto the original strand and repeat the ground state configurations optimization until there are 32 units of chromophores. We duplicate the whole polymer chain with close contact between the chains in Chemdraw 3D. The steric energy between the polymeric chains is minimized using the MM2 Level. We repeat the same procedure until we obtained 8 polymeric chains giving us 256 units of chromophores in cubic arrangement. The same procedure is also applied for the small molecules. The steric energies of an ensemble of molecules/polymers are minimized and terminated when the minimum RMS Gradient is less than 0.100. The ensemble of molecules is then brought up to a target temperature of 300K with a heating rate of 1Kcal/atom/s with a 2.0fs step interval. A program is written in Labview to find the minimum contact distance between two nitrogen atoms in two different molecules. A histogram of minimum contact distance between each of the chromophores (interchromophoric distance) can be plotted.

Result and discussion

Phosphorescence spectra

The chemical structures of materials used in this study are given in Figure 1. In order to understand how each substituent affects the overall molecular triplet energies, we investigated the triplet energies of the substituents. All the compounds studied here, except carbazole monomers, are amorphous. The lack of ability to form crystal is due to the presence of bulky side groups and/or the highly twisted structure.[27,28] Figure 2(a) shows the normalized phosphorescent spectra of carbazole in a dilute form and drop-casted onto thin film. The spectra between the two states are very different. It is important to note that fluorescence and phosphorescent spectra of the solid states are completely different in all cases investigated. There is no delay fluorescence observed. In the dilute phase, the 0-0 vibronic peak is located at 2.98 eV, consistent with published data[22]. However, the spectrum of the drop-casted carbazole thin film is drastically red-shifted by 0.68 eV with the first peak located at 2.30 eV. This is far lower in energy than most triplet excimer emissions obtained from carbazole derivatives.[22,23,29] It could be the result of very strong interactions between carbazole molecules since the drop-casted films are expected to produce polycrystalline carbazole microcrystals. We also observed a second peak located at 1.80 eV of unknown origin.

Figure 2(b) shows the normalized phosphorescent spectra of carbazole functionalized with *tert*-pentyl at the 3 and 6 positions of carbazole in dilute form and drop-casted thin film. The whole spectrum of 3,6-di-tert-pentyl-9H-carbazole is red-shifted by 0.05 eV compared to the monomer in dilute form. However, in the drop-casted thin film, the first peak is increased to

View Article Online
DOI: 10.1039/C5RA09340F

2.58 eV compared to 2.30 eV for carbazole monomers. This indicates that the *tert*-pentyl acts as an bulky substituent, effectively reducing the intermolecular interactions. However the peak at 1.80 eV can be observed with a reduced intensity. By functionalizing carbazole with 3,6-di-tert-pentyl-9H-carbazole at the 3 and 6 positions to give 3,6-bis(3,6-ditert-pentyl-carbazol-9-yl)carbazole (**TPC**), the triplet energy in the dilute form is further reduced from 2.93 eV to 2.81 eV as shown in Figure 2(c). This indicates that the triplet exciton wavefunction might not be fully confined into the monomeric carbazole. Nevertheless, the first peak of the drop-casted thin film has increased to 2.68 eV for **TPC**. Unlike carbazole and 3,6-di-tert-pentyl-9H-carbazole, where the phosphorescence is featureless, phosphorescence from **TPC** contains vibronic features. The difference between the first peak of drop-casted thin film and dilute form (ΔE_{SD}) for **TPC** is reduced to 0.13 eV compared with 0.68 eV and 0.35 eV for carbazole and 3,6-di-tert-pentyl-9H-carbazole respectively. When two **TPC** compounds are coupled at the 1 and 3 position of the benzene ring to give 1,4-bis(3,6-bis(3,6-ditert-pentyl-carbazol-9-yl)carbazol-9-yl)benzene (**TPC-CCP**), the triplet energy in the dilute form is further reduced to 2.78 eV. However, the ΔE_{SD} is reduced to 0.05 eV resulting in the triplet energy in the thin film to be 2.73 eV. The decrease of the triplet energy from 3,6-di-tert-pentyl-9H-carbazole to **TPC** can be explained by the increase of the 'effective' conjugation as evident from the photoluminescence spectra in the dilute solutions as indicated in Figure 3. Even though there is a 'break' of conjugation as a result of the torsional angle between two carbazole substituents for **TPC**, the 'break' is not complete. Depending on the torsional potential, torsional angle and temperature, Boltzmann statistics dictates that there will be a range of possible torsional angles[30]. The torsional angle between two carbazoles is modelled using a Gaussian PM6 resulting in a potential barrier of ~0.2 eV with a torsional angle of 47.4^{o} for **TPC** as shown in Figure 4. Compared with 4,4′-bisBis(9-carbazoleyl)-2,2′-dimethyl-biphenyl (**CBDP**), it has a potential barrier of ~0.8 eV with a torsional angle of 82^{o}. The number of near planar conformations between two carbazoles for **TPC-CCP** can be calculated using Boltzmann distribution[30] (See Supplementary information Fig1). Ideally the torsional potential barrier is significantly higher than the thermal energy and Gaussian disorder. In order to further confirm whether steric hindrance can reduce the ΔE_{SD}, we measure a larger range of compounds. For 3,6-bis(diphenylphosphoryl)-9H-carbazole (**POCARB**) and 2,7-Bis(diphenylphosphoryl)-9,9'-spirobifluorene (**SPPO13**), the role of phosphine oxides is to increase solubility in polar solvents such as alcohol. The diphenylphosphinic moiety/group also increases the intermolecular distance between two

View Article Online
DOI: 10.1039/C5RA09340F

chromosphores. As expected, the ΔE_{SD} is 0.07 eV and 0.06 eV for POCARB and SPPO13 respectively as shown in Figures 5(a) and 5(b). For **PVK**, the monomers being separated by vinyl (two carbons), ΔE_{SD} is 0.29 eV. Poly{3,6-di(t-butyl)-9-[4-(3-methyloxetan-3-ylmethoxy)phenyl]carbazole} (**PtPC**) and poly{9-[4-(3-methyloxetan-3-ylmethoxy)phenyl]carbazole} (**PPC**) are newly synthesized polymers. Both are separated by three carbons and one oxygen atom in the main chain. In **PtPC**, the carbazole is functionalized with *tert*-butyl at the 3 and 6 positions. This results in the reduction of ΔE_{SD} from 0.24eV (**PPC**) to 0.14eV (**PtPC**) as illustrated in Figure 5(c) and 5(d) respectively. We also note that the functionalisation of *tert*-butyl or *tert*-pentyl results in a slight reduction of triplet energy in the dilute form as evident in 3,6-di-tert-pentyl-9H-carbazole and **PtPC**. This can be explained by the effect of hyperconjugation. In terms of the molecular orbital shape of nonsubstituted carbazole, electron distribution is rich at the 3-and 6-positions of the HOMO energy level[31]. The electrons in the sigma bond interact with the π-orbital to give a more extended molecular orbital. The photoluminescence is red-shifted indicating a reduced band-gap and hence reduced triplet energy.

It is clear that the difference in triplet energies measured in the solid states and dilute phases (whether it is triplet excimers from dimers or monomers) must be a function of the distance between two chromophores. (ie, each carbazole in the polymeric chain of **PPC** is distinct from each other as the phosphorescent spectra of **PPC** is very similar to carbazole itself while for example in **TPC**, the carbazoles within the same molecule are not spectroscopically distinct with each other). Here, the minimum distance between two spectroscopically distinct chromophores is referred to as the interchromophoric distance as measured from the nitrogen atom of the chromophore.

Correlation of ΔE_{SD} with interchromophoric distance

Because organic semicoductors are generally amorphous, it is not a trival task to determine how each of the chromophores are separated from each other in an solid state by experimental methods. However, it does not deter some researchers trying to obtain the interchromophoric distance, **r** between two carbazoles using high-level ab initio calculations[32]. The contact distance between two carbazoles in poly(9-vinylcarbazole) (**PVK**) is simulated with more than 200 carbazole units in a given simulation to obtain a statistically meaningful result. An MM2 force field is used. Phosphine oxide is not parameterized within the MM2 and hence not included the calculations. The obtained mean **r** of PVK is 0.39 nm with a standard deviation of 0.05nm. Most **r** have a normal (Gaussian) or log-normal

View Article Online
DOI: 10.1039/C5RA09340F

probability density function (see supplementary information Figure 2). This behaviour has been observed in amorphous solids exhibiting a random network structure[33]. Amorphous organic semiconductors and polymers are disordered and have been shown to exhibit log-normal distributions for interchromophoric distance[34,35]. It is interesting to speculate that such positional disorder distributions might contribute to the Gaussian distribution of the density of states. Figure 6 shows the correlation of ΔE_{SD} with mean **r** for a range of compounds along with their standard deviations. **tpc-CCP** has the largest **r** (1.79 nm) and the largest standard deviation with just slightly less than 10% having **r** less than 1 nm. It is noted here that the **r** for **tpc-CCP** is twice as large as the distance from the nitrogen atom at carbazole to the furthest hydrogen atom at the tert-pentyl substituent (0.85nm). This type of characteristic has been observed in nematic semiconducting liquid crystalline phases exhibiting bulky side groups using X-ray Diffraction[36]. For **TPC**, the **r** is almost half of **tpc-CCP** which is 0.82 nm. It is not surprise since the bulky side groups are on only one side of the carbazole. In the solid states, emission often occurs at lower energies. Hence the red-shifted spectra is observed. Such red shift of energy should depend on the interchromophic distance. Hence, we fit the data with equation below.

$$\Delta E = J_o e^{-2\gamma r} \quad (1)$$

where **r** is the interchromophric distance, γ is the electronic wavefunction localization and J_o is the constant of dimension of energy. Fitting of equation (1) on Figure 5 yields J_o = 1.08 eV, γ = 0.32nm^{-1} with an error of 0.08 eV. These parameters could be used to predict the triplet energies in the solid state for carbazole based materials once the **r** is known. Triplet energies computated in a vacuum using time-dependent density functional theory can be used to predict the triplet states in solid states using this correction[38].

Energy Back transfer

In order to study the effect of energy back transfer between the **Firpic** and solution processable host, we carried out time resolved phosphorescence measurements. 3,5-di(9H-carbazol-9-yl) tetraphenylsilane (**SIMCP2**), 4,4′,4″-tris-(N-carbazolyl)-triphenlyamine (**TcTa**) and **SPPO13** are solution processable hosts which have been used to produce blue phosphorescent organic LEDs [39-41]. The lifetimes of the guest molecules are always used as an indication of the effectiveness of triplet confinement[42,43]. It should exhibit clear monoexponential decay as an indication of good triplet exciton confinement. Time resolved

View Article Online
DOI: 10.1039/C5RA09340F

phosphorescence is carried out on Firpic doped hosts at 10% by weight. The Firpic doped hosts are excited at 400nm. Since the absorption band of the hosts are all less than 370nm, the excitons created by pulsed excitation are Firpic excitons. There is a clear expotential decay of radiative lifetime reducing with increasing triplet energy as measured in solid states as shown in Figure 7. Only **TcTa** shows expontential decay with two lifetimes. Here, we took the longer lifetime as an indication of energy back transfer. The phosphorescence spectra of **SIMCP2** and **TcTa** are given in the supplemtary information Figure S3.

The radiative lifetime of Firpic which is 1.2μs [44] is far longer than the minimum hopping time of a triplet exciton between two molecules which can be as low as a few picoseconds[45]. Assuming that thermal equilibrium is reached between the excited Firpic molecules and the next nearest hosts in the system, the population density between triplet excitons in the Firpic and the host molecules can be calculated using the rate equations:

$$\frac{dn_{Ir}}{dt} = -k_{Ir}n_{Ir} + k_{HE}n_{ho} - k_{EH}n_{Ir} - \gamma_{IR}n_{Ir}^2 \quad (2)$$

$$\frac{dn_{host}}{dt} = -k_{ho}n_{ho} - k_{HE}n_{ho} + k_{EH}n_{Ir} - \gamma_{ho}n_{ho}^2 \quad (3)$$

where n_{Ir} is the triplet exciton population density of Firpic, k_{Ir} is the population decay rate for Firpic, k_{HE} is the transfer rate from the host (H) to the emitter (E), k_{EH} is the transfer rate from the emitter (E) to the host (H), n_{ho} is the triplet exciton population density of the host and k_{ho} is the population decay rate for the host. k_{HE} and k_{EH} are the transfer rates usually given by the Marcus hopping rate for high temperatures or Miller-Abraham for a low temperature regime[46,47]. Since Firpic has a radiative quantum efficency of near 99% ignoring non-radiative decay, k_{Ir} becomes the Einsten A coeffient. k_{ho} is the sum of the radiative and non-radiative decay rates for the triplet excitons of the host molecules located nearest to the Firpic molecules. γ_{ho} and γ_{Ir} are the triplet-triplet annihiation quenching rates for the host and the emitter respectively. The total number of triplet excitons, N, in that system is simply the sum of n_{Ir} and n_{ho}. Maxwell-Boltzmann distribution between energy levels in Firpic and the host molecules can be given as:

$$\frac{n_{Ir}}{n_{ho}} = e^{\frac{E_{ho} - E_{Ir}}{KT}} \quad (4)$$

View Article Online
DOI: 10.1039/C5RA09340F

where E_{ho} and E_{Ir} are the triplet energy levels of the host and Firpic determined in the solid states. E_{ho} and E_{Ir} in equation (4) are the mean values of Gaussian broadened density of states triplet energy levels assuming both have the same variant σ. K is the Boltzmann constant and T is the triplet exciton temperature. Note that the equation 4 does not depend on whether the triplet states originate from the triplet exciton, from a monomer, dimer or excimer, as it is the energy levels which are important as long as the lifetime of the triplet excimers are significantly longer than the Firpic. This is true since phosphorescence from the host can be observed even 800 μs after laser pulse excitation for both doped and undoped host.

Summing equations (2) and (3) gives:

$$\frac{dN}{dt} = -k_{Ir}n_{Ir} - k_{ho}n_{ho} - \gamma_{IR}n_{Ir}^2 - \gamma_{ho}n_{ho}^2 \quad (5)$$

which is independent of the hopping rate given by Marcus and the Miller-Abraham transfer rate. Equation (6) can be further simplified by considering several facts. Firstly, the decay of host triplets is significantly longer than the radiative lifetime of Firpic. Hence $k_{ho}n_{ho} << k_{Ir}n_{Ir}$. Secondly, the fluorination on the ppy ligand of Firpic hinders self-quenching interactions. The photoluminescence quantum yield of Firpic in an inert matrix at concentrations of ≤ 10% has been shown to approach 99%[48]. It is believed that the fluorination on the ppy ligand hinders self-quenching interactions. Hence, the self-quenching of emitter-emitter is too small to have any significant effects. The laser intensity was spread out on a spot of $0.2cm^2$. The initial excitation densities can be calculated from the absorption at 400nm to give an initial exciton density of less than 10^{17} cm^{-3}. However, this exciton density is too small to cause an appreciable host-host quenching.[49] Furthermore, under typical experimental conditions, the low temperature triplet-triplet annihilation rate, γ, is of the order 10^{-14} cm^3/s.[50] This is usually explained by blocked triplet diffusion at extremely low temperatures.[51] Since the experiment is carried out at 77K, this means that $k_{ho}N_{ho}^2 >> \gamma_{ho} N_{ho}^2$ by three order of magnitude. Hence the host-host quenching will not play any significant role.

Equation (5) tends to simplify into:

$$\frac{dN}{dt} = -k_{Ir}n_{Ir} \quad (6)$$

View Article Online
DOI: 10.1039/C5RA09340F

Using equation (4) and keep in mind that $N = n_{Ir} + n_{ho}$ equation (6) becomes:

$$\frac{dN}{dt} = -k_{Ir} \frac{N}{(1 + e^{\frac{E_{Ir} - E_{ho}}{KT}})} \quad (7)$$

Integrating (7) becomes:

$$\tau = \tau_o + (\tau_o e^{\frac{E_{Ir}}{KT}}) e^{\frac{-E_{ho}}{KT}} \quad (8)$$

where τ_o is the radiative lifetime of Firpic embedded in the host. A mono-exponential fit performed for Figure 7 results in τ_o =1.32 μs, an effective temperature of 664 K and a Firpic triplet energy of 2.55 eV. This is higher than the bulk/lattice temperature. The excitons are always coupled with phonons within the molecule. Optical relaxation and the reorganization of the molecular structure from hoping from one molecule to another generate phonons. The high effective temperature might correspond to the vibronic deformation of the ring modes of Firpic[52]. The consequence of equation (4) is that in order to reduce the energy back transfer from the emitter to the host to less than 1%, the hosts must have a triplet energy of at least 0.26 eV higher than the emitters. The equation does not capture the diffusion of the triplet excitons far away from the Firpic–host interface which can result in failed back transfer and hence quenching, as evident from the observed phosphorescence detected with a gate delay of 650μs (see supplementary information Figure 4). It is surprising to see that phosphorescence from Firpic doped hosts are observed except above 2.80eV. The triplet exciton generated by the Firpic molecule can be transferred to the neighbouring host molecule as shown in Figure 8(a). The triplet energy can also be back-transferred to the Firpic molecule. Triplet excitons generated at the host molecules will then undergo random-walks with diffusion taking place in an energetic downward direction and, by thermal excitation, also in an energetic upward direction. Over time, the exciton tends to occupy the tail of the Gaussian density of states resulting in the loss of the triplet exciton as shown in Figure 8(b). Or it might find its way back to the Firpic molecules as shown in Figure 8(c).

Conclusions

View Article Online
DOI: 10.1039/C5RA09340F

The effect of side groups on the energy shift of phosphorescent spectra in the solid state has been quantified. The reduction of energy shifts in the solid state can be related to the increase in interchromophoric distance. By using triplet energies determined in the solid state, we can show clearly that energy transfer between Firpic and the host is governed by the Boltzmann factor. This implies that the host should have a triplet energy greater than 2.80 eV in order to confine the triplet exciton generated in Firpic. This new found understanding will have implications in molecular design for triplet based optoelectronic devices.

Acknowledgements

This research is funded by Chancellery High Impact Research Grant (UM.C/625/1/HIR/195) and (UM.C/625/1/HIR/208) and by Grant No. MIP-024/2013 from the Research Council of Lithuania. S.A. Chen wishes to thank the Ministry of Education and Ministry of Science and Technology of the Republic of China for the financial aid through project NSC-101-2120-M-007-004, NSC-102-2633-M-007-002 and NSC 102-2221-E-007-131

View Article Online
DOI: 10.1039/C5RA09340F

References

1. Q. S. Zhang, T. Komino, S. P. Huang, S. Matsunami, K. Goushi, C. Adachi *Adv. Funct. Mater.*, 2012 , **22** , 2327-2336
2. Z. B. Wang, M. G. Helander, J. Qiu, D. P. Puzzo, Z. H. Lu, *Org. Electron.*, 2012, **13**, 925-931
3. Y. Tao, Q. Wang, C. Yang, J. Qin, D. Ma, *ACS Appl. Mater. Interfaces*,2010, **2**, 2813-2818
4. S. J. Su, E. Gonmori, H. Sasabe, J. Kido, *Adv. Mater. (Weinheim, Ger.)* 2008, **20**, 4189-4194
5. X. F. Ren, J. Li, R. J. Holmes, P. I. Djurovich, S.R. Forrest, M. E. Thompson, *Chem. Mater.* ,2004, **16**, 4743-4747
6. D. N. Congreve, J. Y. Lee, N. J. Thompson, E. Hontz, S. R. Yost, P. D. Reusswig, M. E. Bahlke, S. Reineke, T. Van Voorhis, M. A. Baldo, *Science*, 2013 ,**340**, 334-337
7. P. J. Jadhav, A. Mohanty, J. Sussman, J. Lee, M. A. Baldo, *Nano Lett.*, 2011 ,**11**, 1495-1498
8. J. Lee, P. Jadhav, P. D. Reusswig, S. R. Yost, N. J. Thompson, D. N. Congreve, E. Hontz, T. Van Voorhis, M.A. Baldo, *Acc. Chem. Res.* ,2013 ,**46**, 1300-1311
9. K. Goushi, R. Kwong, J. J. Brown, H. Sasabe, C. Adachi, *J. Appl. Phys.*, 2004 ,**95**, 7798-7802
10. J. H. Seo, N. S. Han, H. S. Shim, S. M. Park, J. H. Kwon, J. K. Song, *Chem. Phys. Lett.* , 2010 ,**499**, 226-230
11. A. Rao, M. W. B. Wilson, J. M. Hodgkiss, S. Albert-Seifried, H. Bassler, R. H. Friend, *J. Am. Chem. Soc.*, 2010 ,**132**, 12698-12703
12. Y.T. Tao, C.L. Yang, J.G. Qin, Chem. Soc. Rev., 2011, **40**, 2943–2970
13. G. D. Scholes, G. R. Fleming, A. Olaya-Castro, R. van Grondelle, *Nat. Chem.*, 2011 ,**3**, 763-774
14. Johnson, J.C., Nozik, A.J. & Michl, J. *Acc. Chem. Res.*, 2013 ,**46**, 1290-1299
15. C. H. Yang, M. Mauro, F. Polo, S. Watanabe, I. Muenster, R. Frohlich, L. De Cola, *Chem. Mater.*, 2012 ,**24**, 3684-3695
16. S. Reineke, T. C. Rosenow, B. Luessem, , K. Leo, *Adv. Mater.*, 2010 ,**22**, 3189-3193
17. I. G. Kaplan ,Theory of Molecular interactions Chap. 1 & 2. (John Wiley & Son, Ltd ,2006)
18. S. Reineke, Baldo, *Sci. Rep.* ,2014 ,**4**, 3797/3791-3797/3798

View Article Online
DOI: 10.1039/C5RA09340F

19. H. D. Burrows, L. J. Hartwell, L. E. Horsburgh, I. Hamblett, S. Navaratnam *Phys. Rev. Lett.*, 2001 ,**86**, 1358-1361
20. D. R. Lee, C. W. Lee, J. Y. Lee, *J. Mater. Chem. C*, 2014 ,**2**, 7256-7263
21. M. Pabst, B. Lunkenheimer, A. Kohn, *J. Phys. Chem. C* ,2011 ,**115**, 8335-8344
22. S. Hashimoto, M. Yamaji, *Phys. Chem. Chem. Phys.*, 2008 ,**10**, 3124-3130
23. S. T. Hoffmann, P. Schrogel, M. Rothmann, R. Q. Albuquerque, P. Strohriegl, A. Kohler, *J. Phys. Chem. B*, 2011 ,**115**, 414-421
24. V. Jankus, A. P. Monkman, *Adv. Funct. Mater.* ,2011 ,**21**, 3350-3356
25. B. Ehrler, B. J. Walker, M. L. Bohm, M. W. B. Wilson, Y. Vaynzof, R. H. Friend, N. C. Greenham, *Nat. Commun.*, 2012 ,**3**, 2012/2011-2012/2016
26. P. J. Jadhav, P. R. Brown, N. Thompson, B. Wunsch, A. Mohanty, S. R. Yost, E. Hontz, T. Van Voorhis, M. G. Bawendi, V. Bulovic, M. A. Baldo, . *Adv. Mater.*, 2012 ,**24**, 6169-6174
27. D. Wagner, S. T. Hoffmann, U. Heinemeyer, I. Munster, A. Kohler, P. Strohriegl, *Chem. Mater.*, 2013, **25** , 3758
28. P. Schrogel, A. Tomkeviciene, P. Strohriegl, S. T. Hoffmann, A. Koehler , C. Lennartz, *J. Mater. Chem.*, 2011, **21**, 2266
29. H. Benten, J. Guo, H. Ohkita, S. Ito, Yamamoto, M; Sakumoto, N; Hori, K; Tohda, Y; Tani, K, *J. Phys. Chem. B*, 2007 ,**111**, 10905-10914
30. W. Barford, *Electronic and Optical Properties of Conjugated Polymers*, Chap. 10,170,(OUP Oxford, 2013).
31. Y. Mizuno, I. Takasu, S. Uchikoga, S. Enomoto, T. Sawabe, A. Amano, A. Wada, T. Sugizaki, J. Yoshida, T. Ono, C. Adachi, *J. Phys. Chem. C*, 2012, **116** , 20681–20687
32. P. De Claire *J. Phys. Chem. B*, 2006 ,**110**, 7334-7343
33. J. F. Shackelford, B. D. Brown, *J. Non-Cryst. Solids*, 1981 ,**44**, 379-382
34. B. Muls, H. Uji-i,, S. Melnikov, A. Moussa, W. Verheijen, J. P. Soumillion, J. Josemon, K. Mullen, J. Hofkens, *ChemPhysChem*, 2005 ,**6**, 2286-2294
35. R. Coehoorn, P. A. Bobbert, *Phys. Status Solidi A*, 2012 ,**209**, 2354-2377
36. K.L Woon, M.P. Aldred, P. Vlachos, G. H. Mehl, T. Stirner, S. M. Kelly, M. O'Neill, *Chem. Mater.* ,2006 ,**18**, 2311-2317
37. M. Kurahashi, M. Fukuyo, A. Shimada, I. Nitta , *Bull. Chem. Soc. Jpn.*, 1969 ,**42**, 2174-2179
38. B.K Ong, K. L.Woon, A. Ariffin, *Synth. Met.*, 2014 ,**195**, 54-60

View Article Online
DOI: 10.1039/C5RA09340F

39. J.S. Chen, C. S. Shi, Q. Fu, F. C. Zhao, Y. Hu, Y. L. Feng, D. G. Ma, *J. Mater. Chem.,* 2012 ,**22**, 5164-5170
40. J-H. Jou; W.B. Wang, S.Z. Chen, J. J. Shyue, M. F. Hsu, C. W. Lin, S.M. Shen, C. J. Wang, C. P. Liu, C.T. Chen, M. F. Wu, S.W. Liu, *J. Mater. Chem.*, 2010 ,**20**, 8411-8416
41. K.H Yeoh, C.Y.B Ng, C. L. Chua, N. AzrinaTalik, K. L. Woon, *Phys. Status Solidi RRL* , 2013 ,**7**, 421-424
42. D. Tanaka, Y. Agata, T. Takeda, S. Watanabe, J. Kido, *Jpn. J. Appl. Phy., Part 2,* 2007 ,**46**, L117-L119
43. Y. Kawamura, K. Goushi, J. Brooks, J. J. Brown, H. Sasabe, C. Adachi, *Appl. Phys. Lett.*, 2005 ,**86**, 071104/071101-071104/071103
44. H.S. Son, C. W. Seo, J.Y. Lee, *J. Mater. Chem.*,2011 ,21, 5638-5644
45. S. T. Hoffmann, S. Athanasopoulos, D. Beljonne, H. Baessler, A. Koehler, *J. Phys. Chem. C* ,2012 ,**116**, 16371-16383
46. Koehler, A.; Baessler, H. *J. Mater. Chem* .,2011 ,**21**, 4003-4011
47. L.S. Devi, M.K. Al-Suti, C. Dosche, M.S. Khan, R.H. Friend, A. Kohler, *Phys. Rev. B: Condens. Matter Mater. Phys.* , 2008 ,**78**, 045210/045211-045210/045218
48. Kawamura , K. Goushi, J. Brooks, J. J. Brown, H .Sasabe, C. Adachi, *Appl. Phys. Lett*, 2005, 86,071104.
49. Ribierre J.C. , Ruseckas A. , Knights K. , Staton S.V. , Cumpstey N. , Burn P.L. , Samuel I.D.W. *Phys. Rev. Lett.* 2008, **100,** 017402
50. Rothe C., Attar H. A. Al, Monkman A. P. *Phys. Rev. Lett. B*, 2005 , **72**, 155330
51. M. Lehnhardt, T. Riedl, T. Rabe, W. Kowalsky *Org. Electron.* , 2011, **12**, 486
52. H.R. Tsai; K.Y. Lu.; S.H. Lai, C.H. Fan, C.H. Cheng, I.C. Chen, *J. Phys. Chem. C* , 2011 ,**115**, 17163-17174

View Article Online
DOI: 10.1039/C5RA09340F

Figure Legends

Figure 1: Molecular structure and the names of materials used in determining the triplet energies.

Scheme 1: Reagents: (a) KI,KIO_3, AcOH,80^oC,24 h; or NBS, toluene, DMF, 0 ^oC; (b) 2-Chloro-2-methylbutane, $AlCl_3$, Dichloromethane(dry),R.T, 24 h; (c)AC_2O,reflux, 4h; (d) Cu_2O DMAc,165^oC, 48 h (e) KOH,DMSO,THF,H_2O,reflux, 4h ; (f)Cu, K_2CO_3,18-Crown-6,*O*-Dichlorobenzene, 180^oC, 24 h or 48 h; (g) H_2O, CH_3CN, μw, 90 ^oC, 1h; (h) $NiCl_2.6H_2O$, Zn, 2,2-bipyridine, 99.5% ethanol, 70 ^oC, 5d.

Figure 2: Phosphorescence spectra in dilute phase or in the form of molecular aggregate formed from drop-casting. ΔE_{SD} is the difference in triplet energies between the two states. All triplet energies are determined from the 0-0 vibronic peak using multi-Gaussian fitting. (a) Carbazole (b) 3,6-di-tert-pentyl-9H-carbazole (c) TPC (d) tpc-CCP.

Figure 3: The normalized photoluminescence emission. The carbazole monomer has a peak at 3.50eV. Substitution of the weak electron donating group decreases the peak to 3.40eV for 3,6-di-tert-pentyl-9H-carbazole. The effective conjugation for TPC and TPC-CCP is larger than carbazole resulting in the red-shift of photoluminescence emission.

Figure 4: The torsional angles for CDBP, TPC and TPC-CCP. The red lines along the molecules in the figure are the measured dihedral angle.

Figure 5: Phosphorescence spectra in dilute form or in the form of molecular aggregate from drop-casting (a) POCARB (b) SPPO13 (c)PPC and (d) PtPC.

Figure 6: Correlation of ΔE_{SD} with mean interchromophoric distance for a range of compounds and the error bars are their respective standard deviation. ΔE_{SD} follows a exp(-2R) decay. ε is the error of fitting. The interchromophoric distance for disordered carbazole is obtained from Ref. 37.

Figure 7: Correlation of the radiative lifetime of Firpic in various hosts. The higher the triplet energy, the shorter the radiative lifetime.

Figure 8: The three main pathways for energy transfer of a triplet exciton generated at the Firpic molecule. (a) Energy transfer between the nearest neighbouring host molecule and the Firpic molecules governed by the Boltzmann factor (b) Down-hill transfer via random

View Article Online
DOI: 10.1039/C5RA09340F

walk away from the Firpic before becoming lost. (c) Multiphonon absorption. The triplet exciton hopped among the host molecules and later finds its way back to the Firpic molecule.

View Article Online
DOI: 10.1039/C5RA09340F

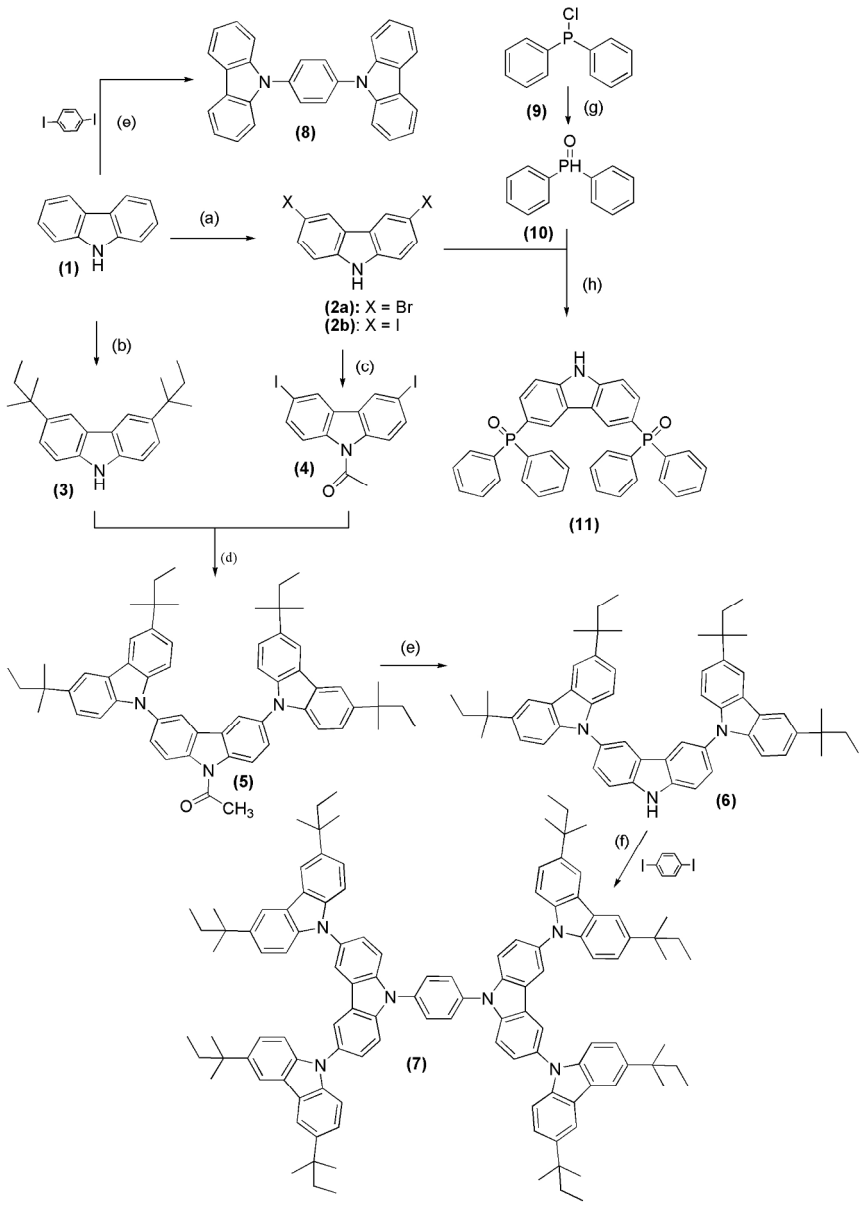

Scheme 1
179x249mm (300 x 300 DPI)

View Article Online
DOI: 10.1039/C5RA09340F

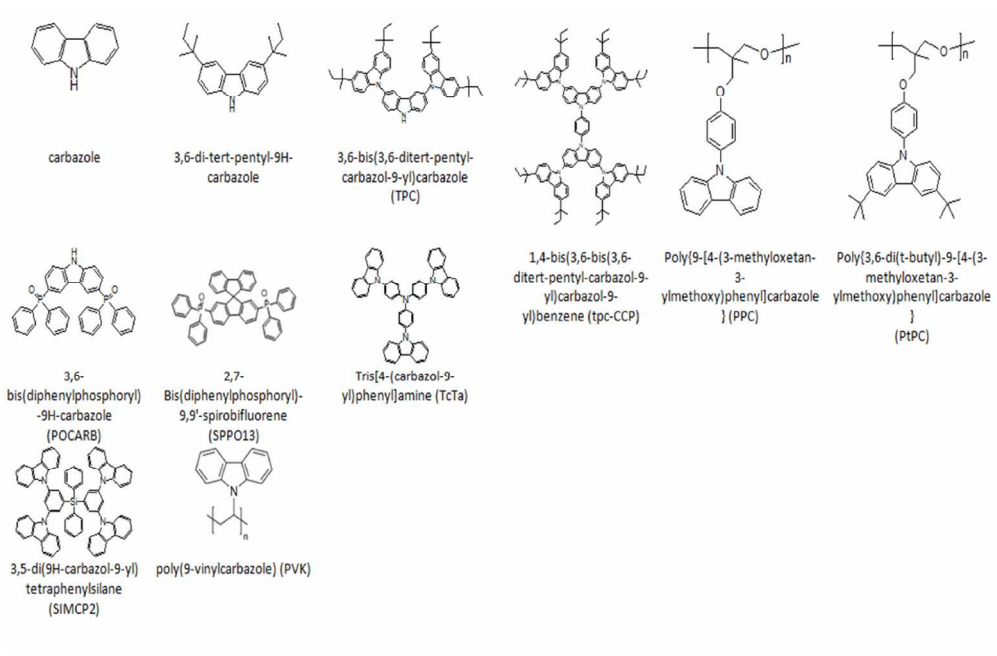

Figure 1
97x63mm (300 x 300 DPI)

View Article Online
DOI: 10.1039/C5RA09340F

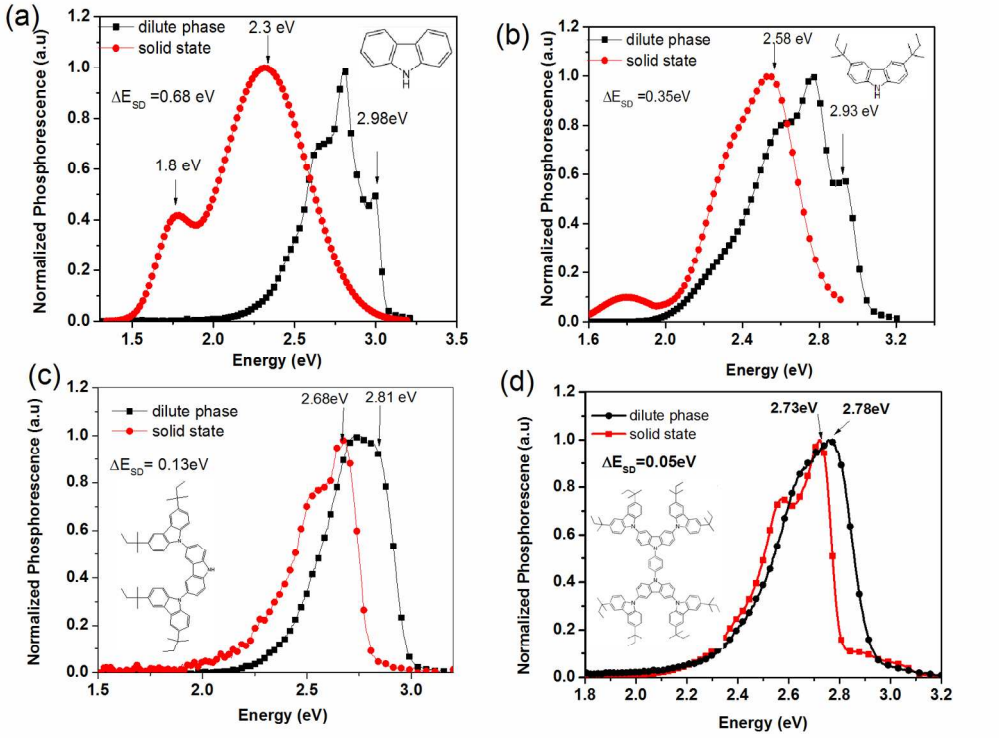

Figure 2
499x383mm (96 x 96 DPI)

View Article Online
DOI: 10.1039/C5RA09340F

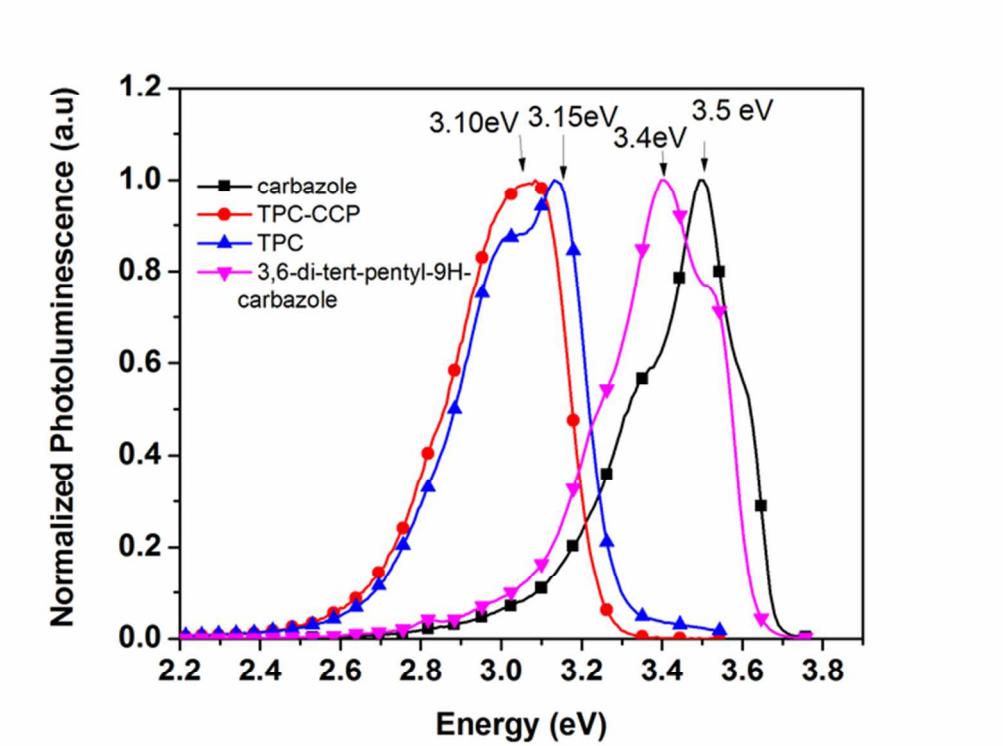

Figure 3
61x47mm (300 x 300 DPI)

View Article Online
DOI: 10.1039/C5RA09340F

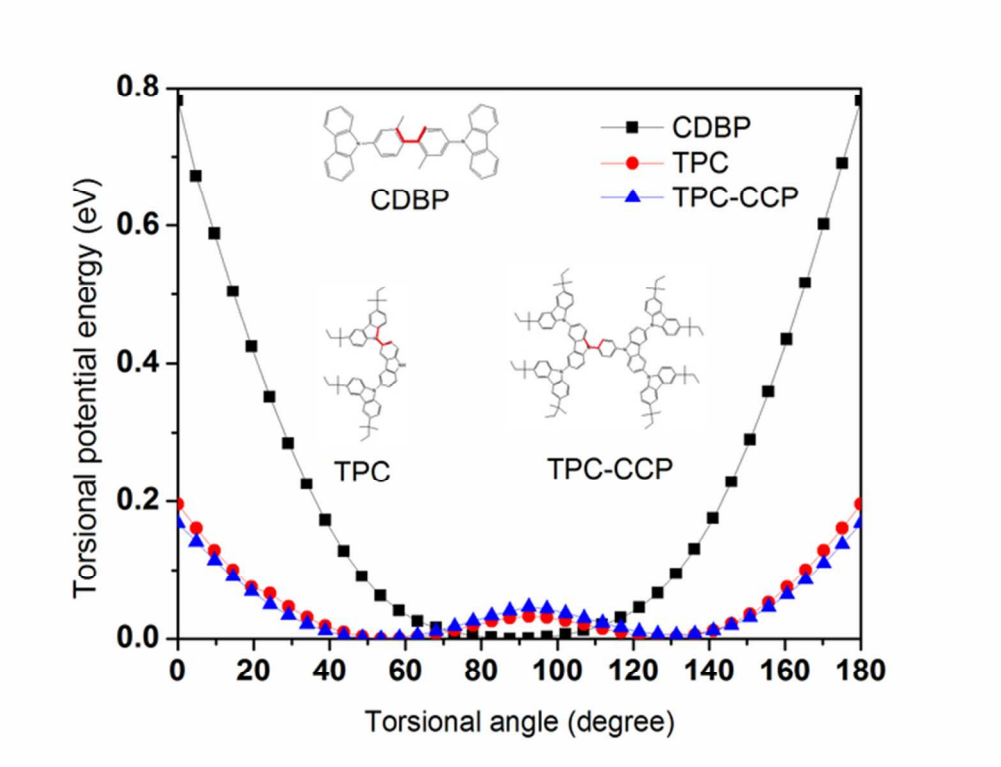

Figure 4
61x47mm (300 x 300 DPI)

View Article Online
DOI: 10.1039/C5RA09340F

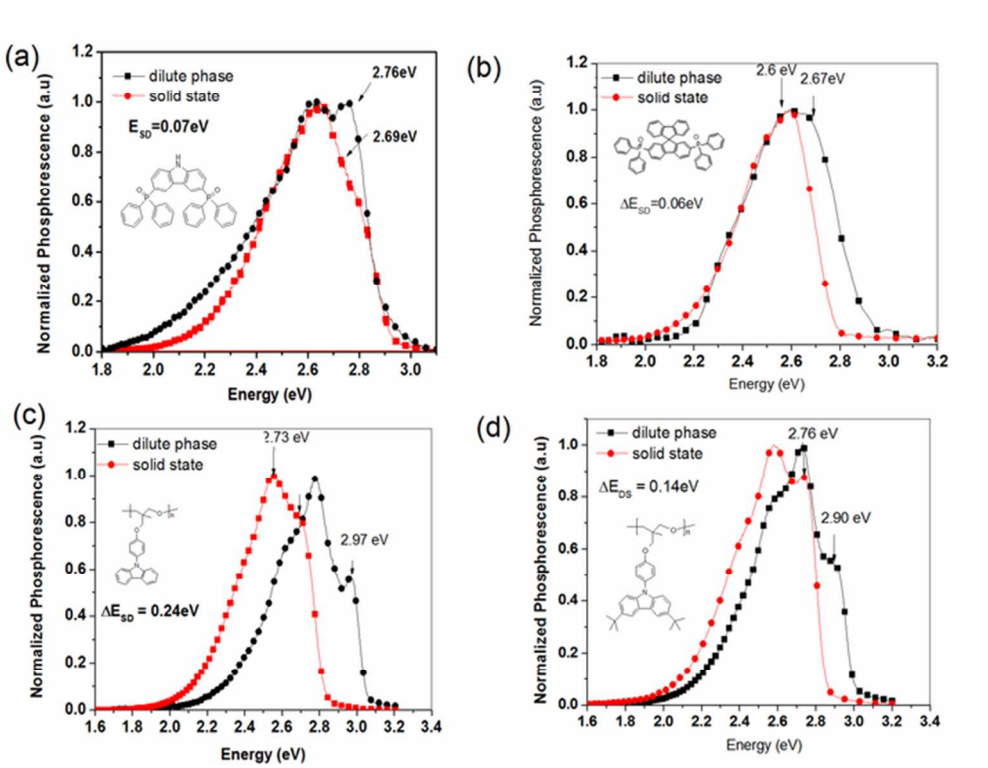

Figure 5
61x47mm (300 x 300 DPI)

View Article Online
DOI: 10.1039/C5RA09340F

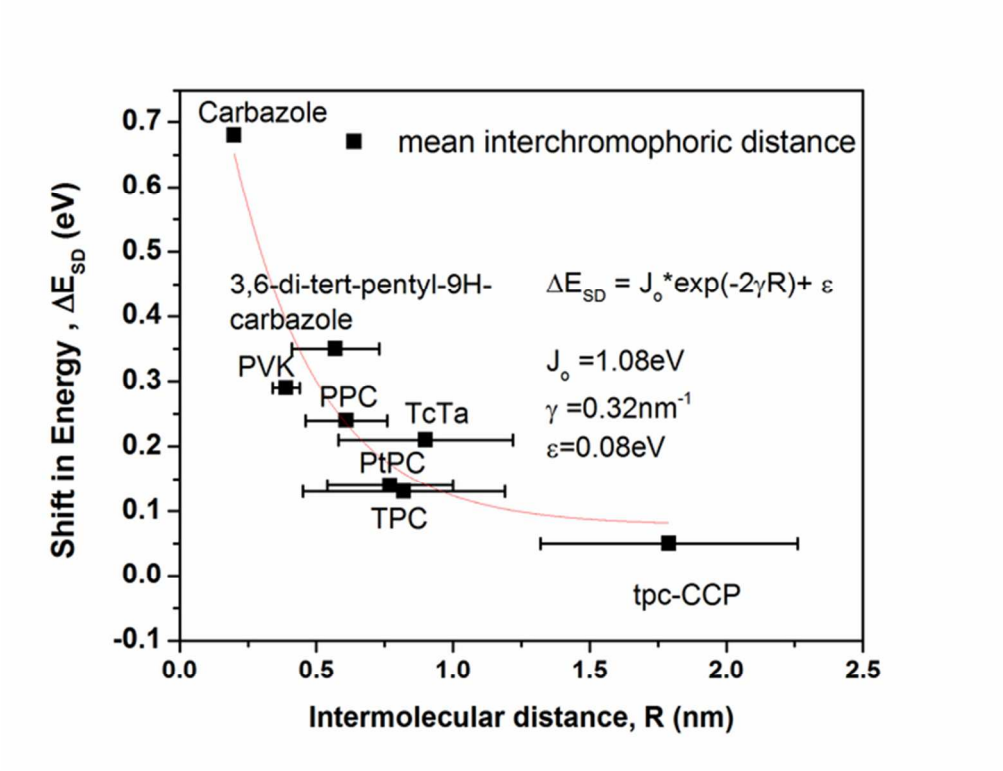

Figure 6
61x47mm (300 x 300 DPI)

View Article Online
DOI: 10.1039/C5RA09340F

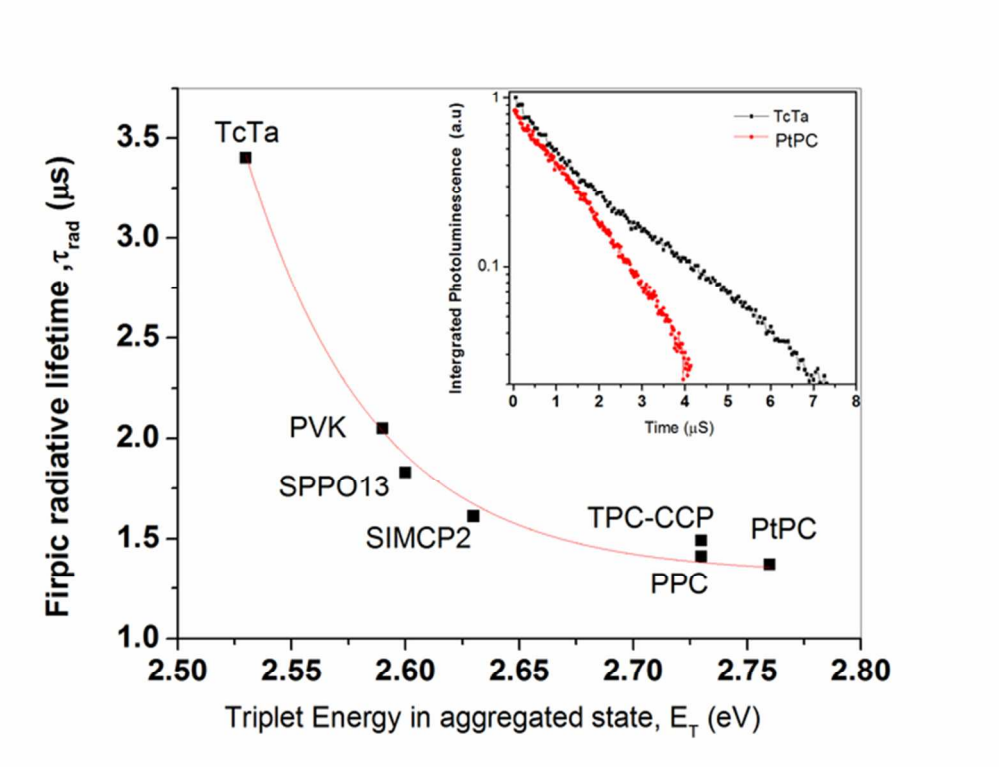

Figure 7
61x47mm (300 x 300 DPI)

View Article Online
DOI: 10.1039/C5RA09340F

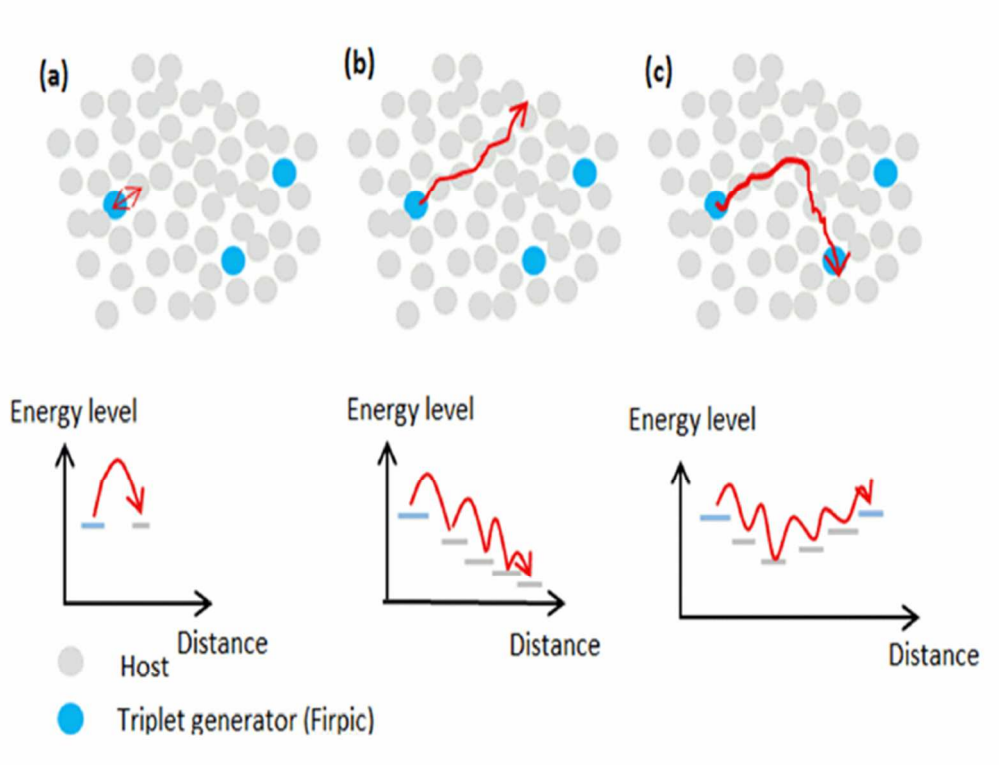

Figure 8
61x47mm (300 x 300 DPI)

View Article Online
DOI: 10.1039/C5RA09340F

Supporting Information

Triplet Energy Confinement and Transfer in Organic Semiconducting Molecular Assemblies

K. L. Woon[1,3], Z. A. Hasan[2,5] , B.K.Ong[2,5], A. Ariffin[2], R. Griniene[4] ,S. Grigalevicius[4] , Show-An Chen[2]

[1]Low Dimensional Material Research Centre (LDMRC), Department of Physics, Faculty of Science, University of Malaya, 50603 Kuala Lumpur, Malaysia

[2]Department of Chemistry, Faculty of Science, University of Malaya, 50603 Kuala Lumpur, Malaysia

[3]Department of Chemical Engineering and Frontier Research Center on Fundamental and Applied Sciences of Matters, National Tsing-Hua University, 101, Section 2, Kuang-Fu Road, Hsinchu 30041, Taiwan, ROC

[4] Department of Polymer Chemistry and Technology, Kaunas University of Technology, Radvilenu Plentas 19, LT-50254 Kaunas, Lithuania

[5] ItraMAS Corporation. Sdn. Bhd., 542A-B Mukim 1, Lorong Perusahaan Baru 2, Kawasan Perindustrian Perai 13600, Penang, Malaysia

1. Materials Synthesis.

3,6-Diiodo-9H-carbazole (2b)[1]

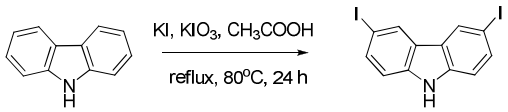

Carbazole (5.0 g, 29.94 mmol) was dissolved in acetic acid (50 ml) and then warmed to 80°C. Potassium iodide (6.51 g, 39.22 mmol) and potassium iodate (4.99 g, 23.35 mmol) was added to this solution and the mixture was refluxed for 24 hours. The crude product was diluted with water and filtered under vacuum. The brown precipitates were stirred in solution of sodium sulfite for 1 hour and filtered with vacuum. The product was recrystallized from dichloromethane to give brownish solid.(9.08 g, 72 %). **Mp** 145-150°C; **IR** (υ_{max}, cm^{-1}): 3412, 1378; **^{1}H NMR** (ppm, 400 Mhz, $CDCl_3$) δ_H : 8.32 (2H, s), 8.10 (1H, s, N-H), 7.69 (2H, dd, *J* = 1.08, 7.40 Hz), 7.22 (2H, d, *J* = 8.48 Hz); **^{13}C NMR** (ppm, 100 Mhz, $CDCl_3$) δ_c : 138.51, 134.82, 129.39, 124.58, 112.69, 82.45 ; **MS (GC) [m/z]:** calcd for $C_{12}H_7I_2N$, 418.87; found, 419.00.

View Article Online
DOI: 10.1039/C5RA09340F

3, 6-Di-*tert*-pentyl-9H-carbazole (3)

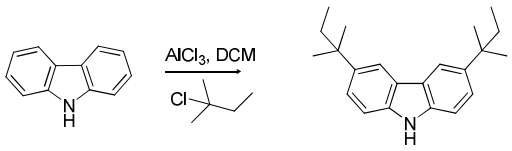

The mixture of carbazole (10.0 g, 59.88 mmol), anhydrous $AlCl_3$ (7.98g, 58.88mmol) and CH_2Cl_2 (200 ml) in a three-necked flask cooled to 0^{o}C was added dropwise a solution of 2-chloro-2-methylbutane (14.75 ml, 119.76 mmol) in CH_2Cl_2 (40 ml). After addition, the mixture was stirred for 10 min at the same temperature. Then the ice bath was removed and the reaction was stirred for 24 hours. The mixture poured into ice-water (500 ml) and extracted with dichloromethane. The combined organic phase was dried over $MgSO_4$. After filtered, the filtration was evaporated to give grey crude which was recrystallized from ethanol to afford white powder (9.33 g, 51%). **Mp** 215-220 °C; **IR** (υ_{max}, cm^{-1}): 3417; 2962; **^{1}H NMR** (ppm, 400 Mhz, $CDCl_3$) δ_H : 8.01 (2H, s), 7.83 (1H, s, N-H), 7.39 (2H, d, *J* = 8.48 Hz), 7.33 (2H, d, *J* = 8.52 Hz), 1.76 (4H, q, *J* = 7.40, 7.44 Hz), 1.41(12H, s), 0.71 (6H, t, *J* = 7.40 Hz); **^{13}C NMR** (ppm, 100 Mhz, $CDCl_3$) δ_c :140.41, 137.96, 124.03, 123.31, 117.06, 109.96, 37.90, 37.42, 29.15, 9.31; **MS (GC) [m/z]:** calcd for $C_{22}H_{29}N$, 307.23; found, 307.00.

***N*-(3, 6-diiodo-9H-carbazol-9-yl)ethanone (4)**

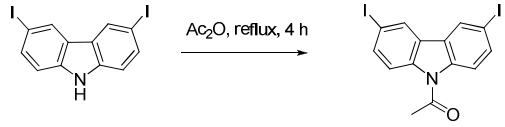

3, 6-Diiodo-9H-carbazole (10 g, 23.87 mmol) was dissolved in acetic anhydride (50 ml). The mixture was refluxed for about 4 hours. The precipitates were filtered under vacuum and wash with water several times to afford white powder (8.76 g, 79 %). **Mp** 215-220°C; **IR** (υ_{max}, cm^{-1}):3062, 1703; **^{1}H NMR** (ppm, 400 Mhz, $CDCl_3$) δ_H : 8.25 (2H, s), 7.96 (2H, d, *J* = 8.80

View Article Online
DOI: 10.1039/C5RA09340F

Hz), 7.78 (2H, d, *J* = 8.80 Hz), 2.84 (3H, s); **^{13}C NMR** (ppm, 100 Mhz, $CDCl_3$) δ_c : 137.95, 136.47, 128.99, 127.19, 118.01, 87.60, 27.68; **MS (GC) [m/z]:** calcd for $C_{14}H_9I_2NO$, 460.88; found, 461.00.

_N_-(3,6-bis(3,6-di-*tert*-pentyl-carbazol-9-yl)carbazole)ethanone (5)

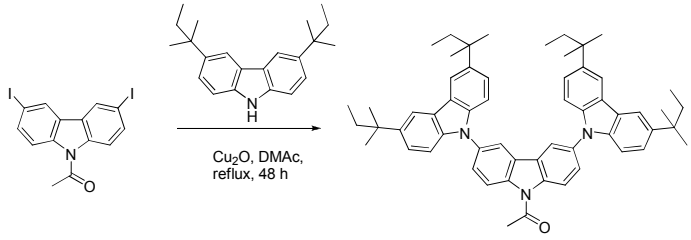

To a solution of 1-(3, 6-diiodo-9H-carbazol-9-yl)ethanone (2.0 g, 4.33 mmol) and 3, 6-Di-*tert*-pentyl-9H-carbazole (2.67, 8.68 mmol) in *N,N*-dimethylacetamide (30 ml) was added copper oxide. The mixture was refluxed for 48 hours and cooled to room temperature and then diluted with water. The precipitates were filtered and recrystallized from ethanol to afford white powder (2.65 g, 74 %). **IR** (υ_{max}, cm^{-1}): 2962, 1702; **^{1}H NMR** (ppm, 400 Mhz, $CDCl_3$) δ_H : 8.49 (2H, d), 8.16 (2H, d), 8.08 (4H, s), 7.75 (2H, dd), 7.37 (8H, m), 3.05 (3H, s), 1.77 (8H, q), 1.42 (24H, s), 0.72 (12H, t); **^{13}C NMR** (ppm, 100 Mhz, $CDCl_3$) δ_c :169.88, 141.17,139.46, 137.74, 134.38, 127.37, 126.71, 124.22, 123.35, 118.39, 117.56, 117.18, 108.92, 37.95, 37.36, 29.12, 27.79, 9.32. **MS (MALDI-TOF) [m/z]:** calcd for $C_{58}H_{65}N_3O$, 819.51; found, 820.1171.

3,6-bis(3,6-di-*tert*-pentyl-carbazol-9-yl)carbazole (6)

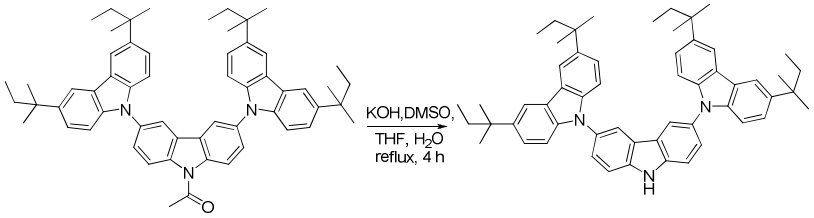

To a solution of *N*-(3,6-bis(3,6-di-*tert*-pentyl-carbazol-9-yl)carbazole)ethanone (2.0 g, 2.44 mmol) in THF (6.0 ml), DMSO (3.0 ml) and water (1.0) was added. The mixture was stirred

View Article Online
DOI: 10.1039/C5RA09340F

for 10 min. KOH (1.2 g, 21.4 mmol) was added subsequently to the mixture and then refluxed for 4 hours. The crude was diluted with water and neutralize with HCl solution (6 N). The crude was filtered and recrystallised from mixture of Hexane : Ethylacetate (1:1) to give white solid. (1.80 g, 95 %). **Mp** 285-290 °C; **IR** (υ_{max}, cm^{-1}): 3453, 2963, 1489; **^{1}H NMR** (ppm, 400 Mhz, $CDCl_3$) δ_H : 8.41 (1H, s, N-H), 8.19 (2H, s), 8.08 (4H, s), 7.67 (4H, m), 7.36 (8H, m), 1.77 (8H, q, *J* = 7.32, 7.44 Hz), 1.42 (24H, s), 0.72 (12H, t, *J* = 7.28 Hz); **^{13}C NMR** (ppm, 100 Mhz, $CDCl_3$) δ_c :140.66, 140.08, 139.01, 130.49, 125.95, 124.11, 124.02, 123.07, 119.42, 117.03, 111.81, 109.04, 37.92, 37.39, 29.15, 9.33; **MS (MALDI-TOF) [m/z]:** calcd for $C_{56}H_{63}N_3$, 777.50; found, 777.6461.

1,4-bis(3,6-bis(3,6-di-*tert*-pentyl-carbazol-9-yl)carbazol-9-yl)benzene (7)

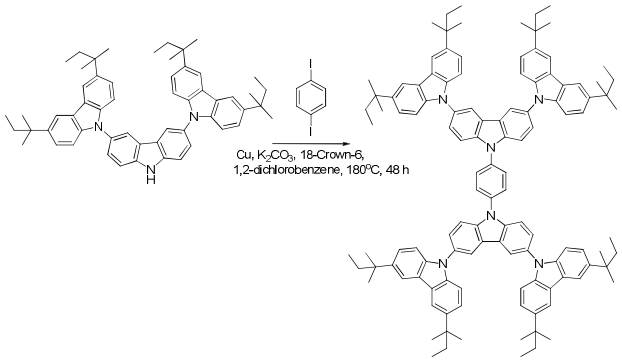

Using a 50 ml two neck round bottom flask with a magnetic stir and a condenser topped with nitrogen inlet. All of the apparatus was purged with nitrogen gas. *O*-dichlorobenzene (10 ml), 3,6-bis(3,6-di-*tert*-pentyl-carbazol-9-yl)carbazole (0.51 g, 0.66 mmol), 1,4-diiodobenzene (0.10 g, 0.30 mmol), K_2CO_3 (0.33 g, 2.40 mmol), Cu powder (0.04 g, 0.60 mmol) and 18-Crown-6 (0.02 g, 0.06 mmol) was added. The mixture was heated at 180°C using oil bath and maintained at that temperature for 48 hours. Cooled the crude mixture and filtered to remove inorganic solid. The filtrate was reduced under high vacuum pump and purify using column chromatography (Hexane: Ethyl acetate; 30:1) to give white powder (0.45 g, 90 %). **IR** (υ_{max}, cm^{-1}):2963, 1489; **^{1}H NMR** (ppm, 400 Mhz, $CDCl_3$) δ_H : 8.32 (4H, d, *J*=1.28 Hz), 8.12 (8H,s), 8.10(4H,s), 7.86 (4H, d, *J*=8.68 Hz), 7.73 (4H, dd, *J* =1.52, 7.12 Hz), 7.41 (8H, d, *J* =9.28 Hz), 7.38 (8H, d, *J*=8.56 Hz), 1.80 (16H, q, *J*=7.28, 7.40 Hz), 1.43 (48H, s), 0.75 (24H, t, *J*=7.28 Hz); **^{13}C NMR** (ppm, 100 Mhz, $CDCl_3$) δ_c : 140.85, 140.20, 140.00, 136.88,

View Article Online
DOI: 10.1039/C5RA09340F

131.39, 128.80, 126.19, 124.32, 124.10, 123.16, 119.50, 117.14, 111.09, 109.01, 37.96, 37.40, 29.16, 9.35; **MS (MALDI-TOF) [m/z]:** calcd for $C_{118}H_{128}N_6$, 1630.02; found, 1630.5803.

1, 4-Di (9H-carbazol-9-yl)benzene (8)[2]

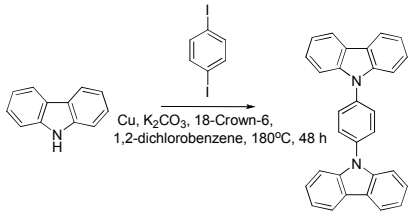

Using a 50 ml two neck round bottom flask with a magnetic stir and a condenser topped with nitrogen inlet. All of the apparatus was purged with nitrogen gas. *O*-dichlorobenzene (5 ml), carbazole (0.22 g, 1.33 mmol), 1,4-diiodobenzene (0.2 g, 0.61 mmol), K_2CO_3 (0.67 g, 4.85 mmol), Cu powder (0.08 g, 1.21 mmol) and 18-Crown-6 (0.032 g, 0.12 mmol) was added. The mixture was heated at 180°C using oil bath and maintained of that temperature for 8 hours. Cooled the crude mixture and filtered to remove inorganic solid. The filtrate was reduced under high vacuum pump and recrystallization using chloroform to afford a white powder (0.13 g, 59%). **Mp** 305-310°C; **IR** (υ_{max}, cm^{-1}): 3056, 1595; **^{1}H NMR** (ppm, 400 Mhz, $CDCl_3$) δ_H : 8.18 (4H, d, *J*=7.6 Hz), 7.81, 4(s, 4H), 7.56 (4H, d, *J*=8.4 Hz), 7.46 (4H, t, *J*=7.6, 7.2 Hz, 7.32 (4H, t, *J*= 7.6 Hz); **^{13}C NMR** (ppm, 100 Mhz, $CDCl_3$) δ_c : 140.77, 136.69, 128.39, 126.13, 123.58, 120.46, 120.28, 109.76; **MS (MALDI-TOF) [m/z]:** calcd for $C_{30}H_{20}N_2$, 408.16; found, 408.2013

3,6-Dibromocarbazole (2a)[3]

A two-neck round-bottom-flask with stir bar was sealed with rubber septum. Air was evacuated with vacuum pump. Nitrogen balloon was inserted. **1** (6.07 g, 36.3 mmol, 1 eq) was dissolved in dry toluene (70 ml) and injected into the reaction flask. A solution of NBS (13.63 g, 76.58 mmol, 2.1 eq) in DMF (35 ml) was injected dropwise into the reaction flask. The reaction was monitored with TLC. The reaction mixture was poured into cold water,

View Article Online
DOI: 10.1039/C5RA09340F

stirred, and seated until precipitation was observed. The white precipitate was filtered, washed with cold MeOH, and recrystallized with MeOH / Hexane (1:5) to give white needle (5.36 g, 46 % yield). Lit. yield = 92 %. m. p. 204-205 **°C**. Lit. m. p. 206-208 **°C**. ^{1}H NMR (400 MHz, Acetone-d6) δ 10.65 (1H, broad s, NH), 8.36 (2H, d, *J* = 1.28 Hz, H4 and H5), 7.55 (2H, dd, *J* = 5.74 and 1.30 Hz, H2 and H7), 7.51 (2H, d, *J* = 5.76 Hz, H1 and H8). ^{13}C NMR (400 MHz, $CDCl_3$) δ 139.2, 128.9, 123.9, 123.2, 113.0, 111.6. ^{1}H NMR and ^{13}C NMR agree to reported values.[4]

Diphenylphosphine oxide (10)

9 (3.0 ml, 16.3 mmol, 1 eq), AR grade acetonitrile (50 ml), water (20 ml) was added to a 100 ml Xpress Plus vessel. The reaction mixture was irradiated with microwave to reach 90 **°C** in 15 min and the temperature was hold for another 15 min. The reaction mixture was allowed to cool to rt. Acetonitrile was removed with rotavap. Extraction with DCM (3 X 50 ml) and water (10 ml) was done. The collected organic layer was dried with MgSO4 and concentrated. The crude product was purified with flash column (EtOAc/Hexane, 1:1) to give clear light yellow liquid (2.47 g, 74% yield). ^{1}H NMR (CDCl3, 400 MHz) δ 8.69 (s, 1H), 7.74-7.68 (m, 4H), 7.60-7.48 (m, 6H), ^{1}H NMR agrees to reported values.[5]

3,6-Bis-(diphenylphosphinyl)-9*H*-Carbazole (11)[6]

In a 50 ml round-bottom-flask, **2a** (1.28 g, 3.9 mmol, 1 eq), **10** (3.59 g, 17.7 mmol, 4.5 eq), nickel(II) chloride hexahydrate (467.7 mg, 1.97 mmol, 0.5 eq), Zinc dust (1.10 g, 16.8 mmol, 4.3 eq), bipyridine (311.6 mg, 2.0 mmol, 0.5 eq) and 99.5% ethanol (10 ml) were added. The reaction mixture was heated to 70 **°C** for 5 days. The reaction mixture was then concentrated with rotavap and diluted with DCM. Extraction was done with DCM (3 X 50 ml). The organic layers are dried with MgSO4 and concentrated. Flash column was done. The product was eluted with 1:20 MeOH:EtOAc. Yield = 1.40 g, 63%. Lit. yield = 74%. ^{1}H NMR (CDCl3, 400 MHz) δ 11.78 (br s, 1 H), 8.31 (d, *J* = 12.44, 2H) 7.68-7.58 (m, 10 H), 7.49-7.7.40 (m, 14 H). ^{13}C NMR (400 MHz, $CDCl_3$) δ 142.9 (d, *J* = 2.2 Hz), 132.9 (d, *J* =104.3 Hz), 132.1,

View Article Online
DOI: 10.1039/C5RA09340F

132.0 129.3 (d, *J* = 11.7 Hz), 128.6 (d, *J* = 11.7 Hz), 125.3 (d, *J* =11 Hz), 122.7 (d, *J* =14.6 Hz), 121.3 (d, *J* = 109.3 Hz), 111.0 (d, *J* = 13.8 Hz). ^{1}H NMR and ^{13}C NMR agree to reported values.

Synthesis of poly{3,6-di(t-butyl)-9-[4-(3-methyloxetan-3-ylmethoxy)phenyl]carbazole} (PtPC) and poly{9-[4-(3-methyloxetan-3-ylmethoxy)phenyl]carbazole} (**PPC**)

The monomers (**4** and **9**) used for preparation of the polymers **PtPC** and **PPC** were synthesized by a multi-step synthetic route as shown in Scheme **1S**. Carbazole-based aldehydes **2** and **7** were synthesized from 9H-carbazole (**1**) and 3,6-di-(tert-butyl)carbazole (**2**), correspondingly, according to the procedures outlined in literature[7] . The hydroxymethyl group containing compounds **3** and **8** were obtained by the reduction of the aldehydes (**2** and **7**) with sodium borohydride in methanol. The compounds **3** and **8** were then converted to the oxetane-based monomers **4** and **9** by their reactions with an excess of 3-bromomethyl-3-methyl-oxetane under basic conditions. The oxetanyl-functionalized monomers were used for the synthesis of polymers **PPC** (**5**) and **PtPC** (**10**) by cationic ring-opening polymerization. The monomers were subjected to polymerization in 1,2-dichlorethane solutions using $BF_3{\cdot}O(C_2H_5)_2$ as an initiator. Low-molecular-weight fractions were removed from the products of polymerization by Soxhlet extraction with methanol.

PPC

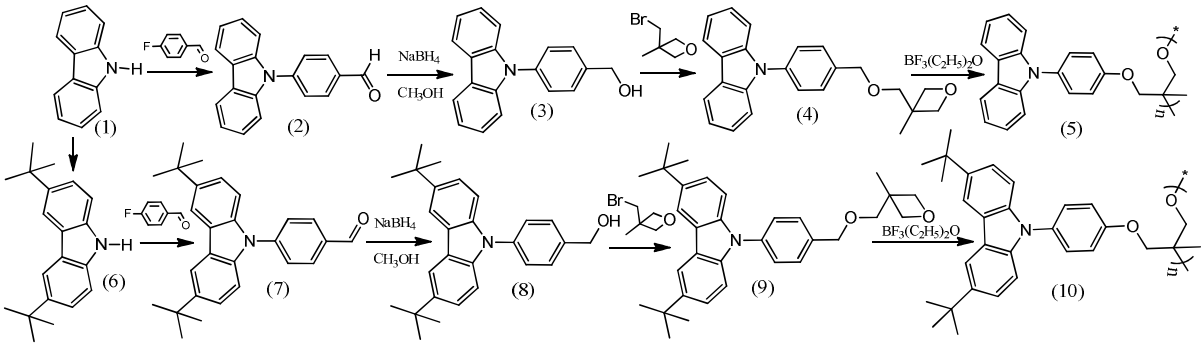

PtPC

View Article Online
DOI: 10.1039/C5RA09340F

Scheme 1S

Experimental details for the synthesis

9H-carbazole, 4-fluorobenzaldehyde, tetra-n-butylammonium hydrogen sulfate (TBAS), $NaBH_4$ and boron trifluoride diethyl etherate [$BF_3{\cdot}O(C_2H_5)_2$] were purchased from Aldrich and used as received. 3-Bromomethyl-3-methyloxetane was bought from Chemada Fine Chemicals (Israel) and used without further purification.

4-(Carbazol-9-yl)benzaldehyde (**2**)[7], 9-{4-(hidroxymethyl)phenyl-1-yl}carbazole **(3)**[8] and 3,6-di(tert-butyl)-9H-carbazole **6**[9] were synthesized according to the procedures outlined in literature.

9-{4-(3-methyloxetan-3-ylmethyl oxymethyl)phenyl-1-yl}carbazole (4).

9-{4-(hidroxymethyl)phenyl-1-yl}carbazole **(3)** (2 g, 7.3 mmol) was dissolved in 10 ml of acetone and 3-bromomethyl-3-methyl-oxetane (2.4 g, 14 mmol) was added. The mixture was heated to 60 ◦C and KOH (1.24 g, 22 mmol), K_2CO_3 (0.96 g, 7.3 mmol) and a catalytic amount of TBAS were added to it by small portions. The reaction mixture was stirred at 60 ◦C for 2 h. When the reaction was finished (TLC control), the mixture was filtered off and the solvent was evaporated under reduced pressure. The crude product was purified by silica gel column chromatography using hexane/ethyl acetate (vol. ratio 4:1) as an eluent. Yield: 1.7 g (65 %) of material 4. M.p.: 95 ^oC (DSC). ^1H NMR spectrum (400 MHz, $CDCl_3$, δ, ppm): 8.14 (d, 2H, J = 7.6 Hz, Ar); 7.56 (d, 4H, J = 7.8 Hz, Ar); 7.42 - 7.40 (m, 4H, Ar); 7.31 - 7.27 (m, 2H, Ar); 4.69 (s, 2H, $PhCH_2$); 4.59 (d, 2H, J = 5.6 Hz, CH_2 of oxetane ring); 4.43 (d, 2H, J = 6.2 Hz, CH_2 of oxetane ring); 3.64 (s, 2H, OCH_2); 1.40 (s, 3H, CH3). IR (KBr, cm−1): 3048 (C-H, Ar); 2951, 2925, 2865 (C-H); 1624, 1594, 1573 (C=C Ar); 1516, 1478, 1452 (C=C, Ar and C-H); 1334, 1315, 1234 (C-N, Ar); 1106 (C-O-C, of oxetane ring); 1094, 980, 972 (C-O-C); 836, 824, 748, 724 (C-H Ar).

Poly{9-[4-(3-methyloxetan-3-ylmethoxy)phenyl]carbazole} (PPC) (5). 9-{4-(3-methyloxetan-3-ylmethyl oxymethyl)phenyl-1-yl}carbazole (**4**) (1.4 g, 3.9 mmol) was dissolved in 7.8 ml of dichloroethane under nitrogen. Then $BF_3{\cdot}O(C_2H_5)_2$ (0.12 mmol, 14.5 µl) was added to the solution and the reaction mixture was stirred for 24 h at 60 ^oC under nitrogen. After the reaction the initiator was neutralized by ammonia solution (26%). Then

View Article Online
DOI: 10.1039/C5RA09340F

the solvent was removed by evaporation. The product was dissolved in a small amount of chloroform and precipitated into methanol. After Soxhlet extraction (24 h) by methanol and re-precipitation, the yield of polymer **5** was 1.3 g (93%). M_n = 22700, M_w = 26400**.** ^{1}H NMR spectrum (400 MHz, $CDCl_3$, δ, ppm): 8.13 - 8.91 (m, 2H, Ar); 7.53 – 7.17 (m, 10H, Ar); 4.64 – 4.39 (m, 2H, $PhCH_2$); 3.55 – 3.18 (m, 6H, OCH_2); 1.10 – 0.85 (m, 3H, CH_3). IR (KBr, cm^{-1}): 3046 (C-H, Ar); 2961, 2854 (C-H); 1625, 1607, 1597 (C=C, Ar); 1516, 1479, 1452 (C=C, Ar and C-H); 1361, 1334, 1316 (C-N, Ar); 1094 (C-O-C); 748, 723 (C-H Ar).

4-(3,6-di-tert-butylcarbazol-9-yl)benzaldehyde (7) To a stirred 3,6-di-tert-butylcarbazole (3.6 g, 12.9 mmol), potassium tert-butoxide (2.48 g, 25.8 mmol) in 15ml of anhydrous DMF , 4-fluorobenzaldehyde (2.78 ml, 19.3 mmol) was added slowly. The mixture was heated at 110 ^{o}C for 2 h. The resulting mixture was poured in ice-water. The mixture was filtered and evaporated. The crude product was purified by silica gel column chromatography using the mixture of ethyl acetate and hexane (vol. ratio 1:30) as an eluent. Yield: 2.2 g (44 %) of yellow solid. ^{1}H NMR spectrum (400 MHz, $CDCl_3$, δ, ppm): 10.1 (s, 1H, -CHO); 8.16 (s, 2H, Ar); 8.11 (d, 2H, J = 8,4 Hz, Ar); 7.79 (d, 2H, J = 8,4 Hz, Ar); 7.50 (dd, 2H, J_1 = 1.6 Hz, J_2 = 8.4 Hz, Ar); 7.46 (d, 2H, J = 8.8 Hz, Ar); 1.48 (s, 18H, CH_3). IR (KBr, cm^{-1}): 2959, 2906, 2865 (C-H); 2827, 2734 (C-H, CHO gr); 1698 (C=O, CHO gr.); 1600 (C=C Ar); 1513, 1488, 1472, 1451 (C=C, Ar and C-H); 1368 (C-H, $C(CH_3)_3$ gr.); 1325, 1297 (C-N, Ar); 875, 841, 818 (C-H Ar).

9-(4-{hidroksimethyl}phenyl-1-yl)-3,6-di-tret-buthylcarbazole (8) was synthesized as follows. Compound **6** (0.9 g, 2.35 mmol) was dissolved in 9 ml methanol. $NaBH_4$ (0.1 g, 2.65 mmol) was added to the solution. The resulting mixture was refluxed for 0.5 h. Then the reaction mixture was poured into ice-water. The product was extracted by chloroform. The combined extract was dried over anhydrous Na_2SO_4. The crude product was purified by silica gel column chromatography using the mixture of ethyl acetate and hexane (vol. ratio 1:4) as an eluent. Yield: 0.88 g (98 %) of material **8**. ^{1}H NMR spectrum (400 MHz, $CDCl_3$, δ, ppm): 8.14 (d, 2H, J = 1.6 Hz, Ar); 7.58 (d, 2H, J = 8,8 Hz, Ar); 7.55 (d, 2H, J = 8.8 Hz, Ar); 7.46 (dd, 2H, J_1 = 2.0 Hz, J_2 = 8.4 Hz, Ar); 7.34 (d, 2H, J = 8.4 Hz, Ar); 4.83 (s, 2H, CH_2); 1.65 (s, 1H, OH), 1.47 (s, 18H, CH_3). IR (KBr, cm^{-1}): 3271 (O-H); 2953, 2901, 2865 (C-H); 1609 (C=C Ar); 1516, 1489, 1474 (C=C, Ar and C-H); 1369, 1364 (C-H, $C(CH_3)_3$ gr.); 1295, 1263 (C-N, Ar); 880, 849, 811 (C-H Ar).

View Article Online
DOI: 10.1039/C5RA09340F

3,6-Di(t-butyl)-9-[4-(3-methyloxetan-3-ylmethoxy)phenyl]carbazole (4). 9-(4-9-(4-{hidroksimethyl}phenyl-1-yl)-3,6-di-tret-buthylcarbazole (1.0 g, 2.6 mmol) was dissolved in 10 ml of acetone and 3-bromomethyl-3-methyl-oxetane (1.2 g, 7.3 mmol) was added. The mixture was heated to 60 ◦C and KOH (0.5 g, 8.9 mmol), K_2CO_3 (0.4 g, 3.1 mmol) and a catalytic amount of TBAS were added to it by small portions. The reaction mixture was stirred at 60 ◦C for 2 h. When the reaction was finished (TLC control), the mixture was filtered off and the solvent was evaporated under reduced pressure. The product was crystallized from methanol. Yield: 1.1 g (66 %) of white crystals. M.p.: 127 ^{o}C (DSC). ^{1}H NMR spectrum (400 MHz, $CDCl_3$, δ, ppm): 8.18 (d, 2H, J = 1.6 Hz, Ar); 7.56 (s, 4H, Ar); 7.47 (dd, 2H, J_1 = 2.0 Hz, J_2 = 8.8 Hz, Ar); 7.37 (d, 2H, J = 8.8 Hz, Ar); 4.70 (s, 2H, $PhCH_2$); 4.61 (d, 2H, J = 5.6 Hz, CH_2 of oxetane ring); 4.44 (d, 2H, J = 6.2 Hz, CH_2 of oxetane ring); 3.64 (s, 2H, OCH_2); 1.48 (s, 18H, $C(CH_3)_3$); 1.41 (s, 3H, CH3). IR (KBr, cm−1): 3048 (C-H, Ar); 2959, 2905, 2869 (C-H); 1624 (C=C Ar); 1516, 1493, 1473 (C=C, Ar and C-H); 1370, 1363 (C-H, $C(CH_3)_3$ gr.); 1298, 1265, 1239 (C-N, Ar); 1082, 977 (C-O-C); 847, 837, 712 (C-H, Ar).

Poly{9-[4-(3-methyloxetan-3-ylmethoxy)phenyl]carbazole} (PPC, 10) 9-(3-methyloxetan-3-ylmethyl)-3,6-di-tret-buthylcarbazole (**4**) (0.7 g, 1.5 mmol) was dissolved in 3.0 ml of dichloroethane under nitrogen. Then $BF_3{\cdot}O(C_2H_5)_2$ (0.04 mmol, 5.5 µl) was added to the solution and the reaction mixture was stirred for 24 h at 60 ^{o}C under nitrogen. After the reaction the initiator was neutralized by ammonia solution (26%). Then the solvent was removed by evaporation. The product was dissolved in a small amount of chloroform and precipitated into methanol. After Soxhlet extraction (24 h) by methanol and re-precipitation, the yield of polymer 10 was 0.54 g (78%). Mn = 14300, Mw = 21700**.** ^{1}H NMR spectrum (400 MHz, $CDCl_3$, δ, ppm): 8.14 - 8.04 (m, 2H, Ar); 7.55 – 7.15 (m, 8H, Ar); 4.65 – 4.42 (m, 2H, $PhCH_2$); 3.52 – 3.16 (m, 6H, OCH_2); 1.51 – 1.32 (m, 18H, $C(CH_3)_3$); 1.06 – 0.95 (m, 3H, CH_3).

View Article Online
DOI: 10.1039/C5RA09340F

2. Supplementary Figures

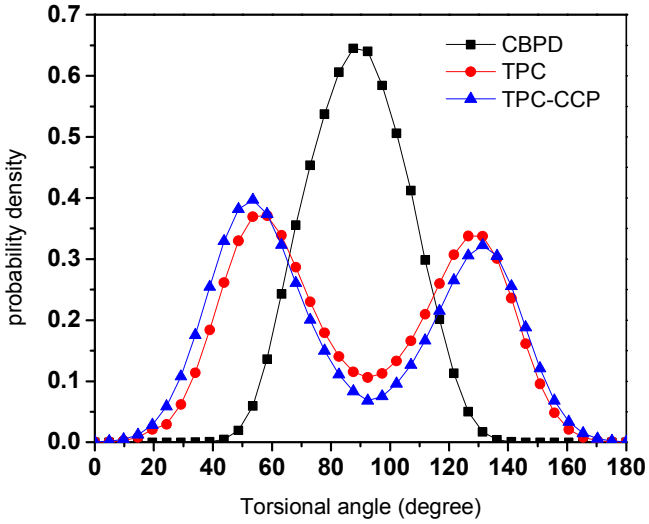

Supplementary Figure 1: Probability density distribution of torsional angle as predicted by Boltzmann distribution for free rotating unit. Less than 1% of TPC and TPC-CCP molecules have torsional angle less than 20^{o}. This will increase the electronic wave function overlap between two chomophores separated by the torsional twist. For CBPD molecules, the torsional angle is highly confined in the range of 40^{o} to 130^{o}. This means that the carbazoles separated by the twist are effectively spectroscopically distinct.

View Article Online
DOI: 10.1039/C5RA09340F

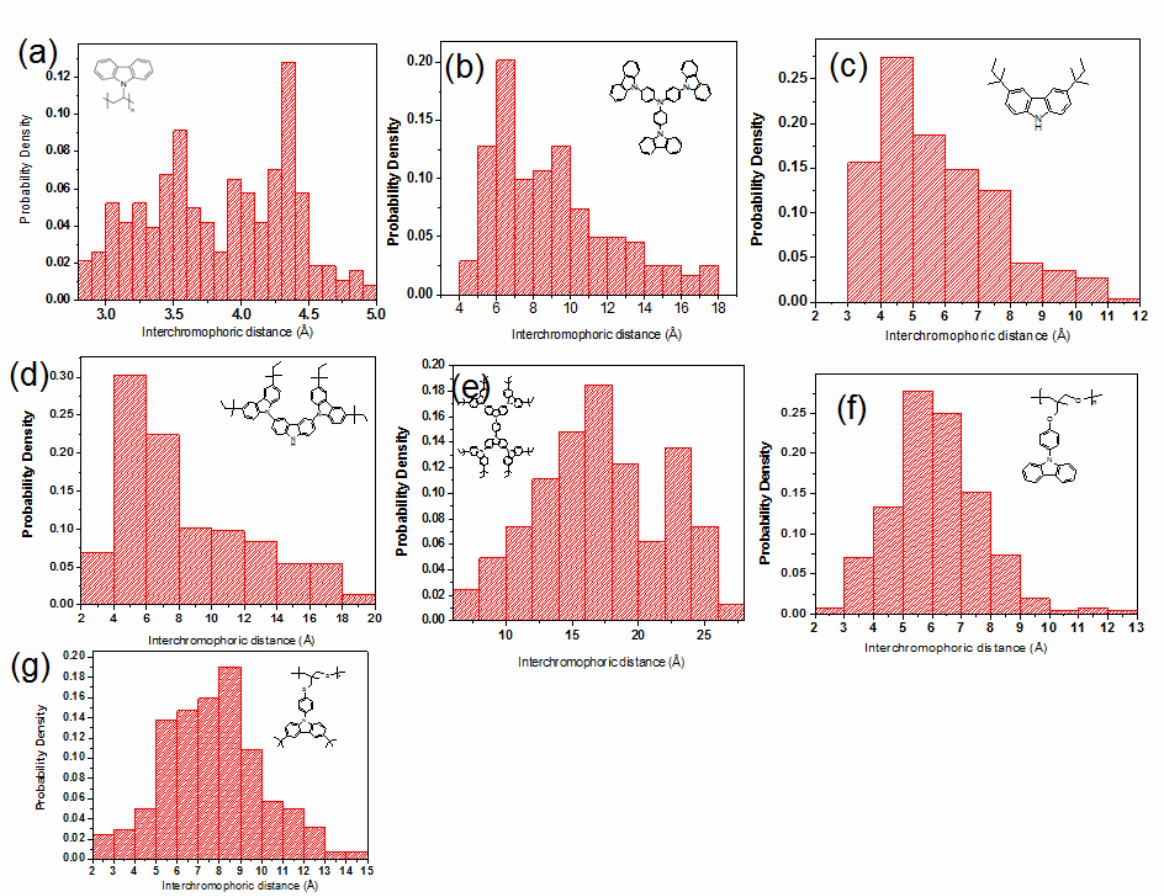

Supplementary Figure 2: Probability density distribution of the interchromophoric distance. Note that most of the interchromophoric distances exhibit lognormal distributions.

View Article Online
DOI: 10.1039/C5RA09340F

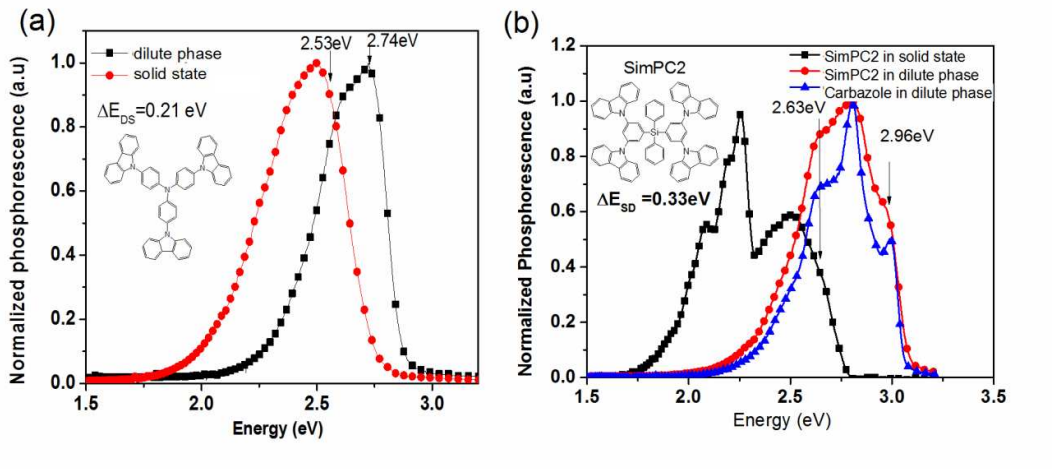

Supplementary Figure 3: The phosphorescence spectra of (a) TcTa and (b) SimPC2.

View Article Online
DOI: 10.1039/C5RA09340F

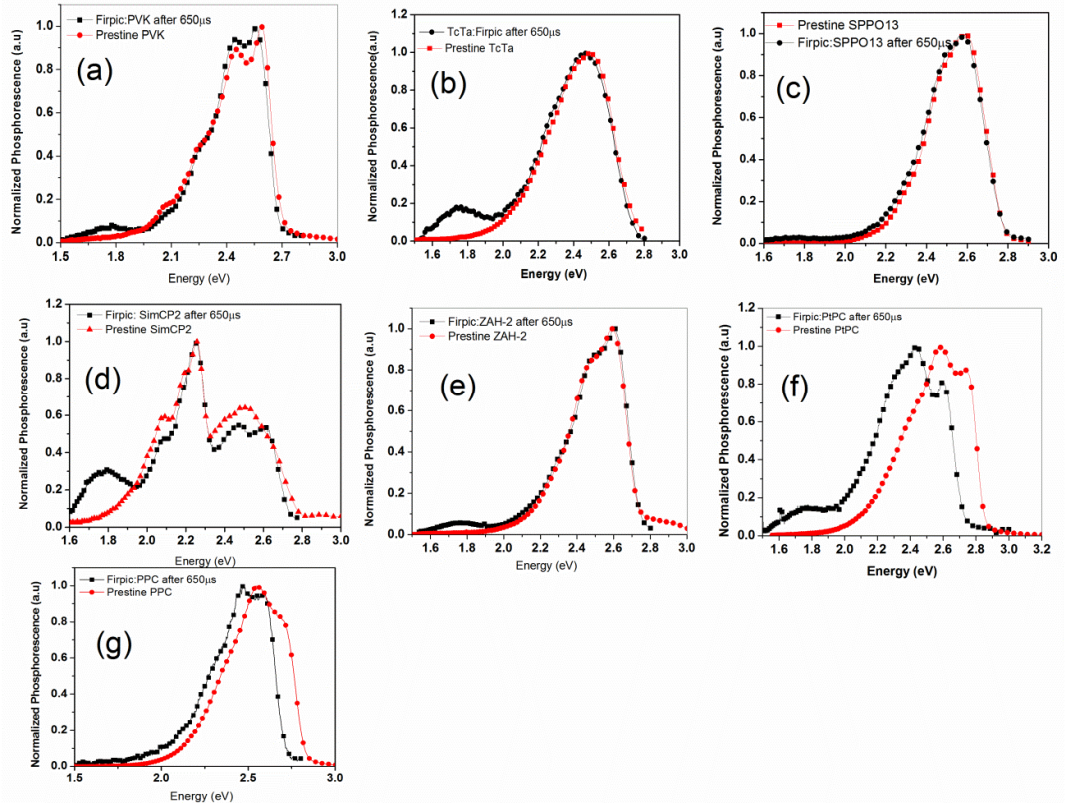

Supplementary Figure 4: Phosphorescence of Firpic doped hosts. The emission is dominated by Firpic (not shown here) within time window of 10μs after the pulse excitation at 400nm. Phosphorescence of the host from the Firpic doped hosts can still be detected albeit very weak with a gate delay of 650µ. (a)-(e)The phosphorescence are very similar to the host emission without Firpic except there is a peak observed at 1.8eV. (f) and (g) the phosphorescence of the Firpic doped host is very different from the prestine host emission in terms of shift of spectra. No phosphorescence is observed above 2.8eV.

1. H.R. Tsai, K.Y. Lu.; S.H. Lai, C.H. Fan, C.H. Cheng, I.C. Chen, *J. Phys. Chem. C* , 2011 ,**115**, 17163-17174

View Article Online
DOI: 10.1039/C5RA09340F

References:

1. A. Kimoto, J-S Cho, M. Higuchi, K. Yamamoto, *Macromolecules*, 2004, **37**, 5531-5537.
2. P. Schroegel, A. Tomkevičienė , S.T. Hoffmann, A. Köhler, C. Lennartz *J. Mater. Chem.* , 2011, **21**, 2266-2273.
3. Ku C.-H., Kuo C.-H, Chen C.-Y, Leung M.-K., Hsieh K.-H., *J. Mater. Chem.* 2008, **18**, 1296-1301.
4. K. Smith, D. M. James, A. G. Mistry, M. R. Bye, D. J. Faulkner, *Tetrahedron* 1992**, 48***, 7479-7488.*
5. T. H. Woeste, M. Oestreich, *Chem. Eur. J.* 2011, **17**, 11914-11918.
6. X.-H. Zhang, H.-Z. Liu, X.-M. Hu, G. Tang, J. Zhu, Y.-F. Zhao, *Org. Lett.* 2011, **13**, 3478-3481.
7. T. Sun, Y. L. Pan, J. Y. Wu, H. P. Zhou, Z. Z. Zhao, Y. P. Tian, Trans. Met. Chem. 2007, **32**, 449 .
8. R. Paspirgelyte , J.V. Grazulevicius, S. Grigalevicius, V. Jankauskas. Reactive & Functional Polymers. 2009, **69**, 183–188.
9. T. H. Xu, R. Lu, X. L. Liu, X. Q. Zheng, X. P. Qiu and Y. Y. Zhao, Org. Lett. 2007, **9**, 797.